Peptide Ancestry Informative Markers in Uterine Neoplasms from Women of European, African and Asian Ancestry

Nicholas W. Bateman, PhD*[1-3], Christopher M. Tarney, MD[1], Tamara S. Abulez, BS[1,3], Brian L. Hood, PhD[1,3], Kelly A. Conrads, PhD[1,3], Ming Zhou, PhD[4], Anthony R. Soltis, PhD[3,5], Pang-ing Teng, PhD[1,3], Amanda Jackson, MD[1], Chunqiao Tian, PhD[1,3], Clifton L. Dalgard, PhD[5,6], Matthew D. Wilkerson, PhD[2,3,5,6], Michael D. Kessler, PhD[7], Zachary Goecker, PhD[8], Jeremy Loffredo, BS[1], Craig D, Shriver, MD[2], Hai Hu, PhD[9], Michele Cote, PhD[10], Glendon J. Parker, PhD[8], James Segars, MD[11], Ayman Al-Hendy, MD, PhD[12], John R. Risinger, PhD[13], Kathleen M. Darcy, PhD[1-3], Yovanni Casablanca, MD[1,2], G. Larry Maxwell, MD[1,2,4], Thomas P. Conrads, PhD[1,2,4], Timothy D. O'Connor, PhD*[6,14,15]

[1]Gynecologic Cancer Center of Excellence, Department of Obstetrics and Gynecology, Uniformed Services University and Walter Reed National Military Medical Center, 8901 Wisconsin Avenue, Bethesda, MD 20889, USA.

[2]The John P. Murtha Cancer Center, Uniformed Services University and Walter Reed National Military Medical Center, 8901 Wisconsin Avenue, Bethesda, MD 20889, USA.

[3]Henry M. Jackson Foundation for the Advancement of Military Medicine, Inc., 6720A Rockledge Dr., Suite 100, Bethesda, MD 20817, USA.

[4]Department of Obstetrics and Gynecology, Inova Fairfax Medical Campus, 3300 Gallows Rd. Falls Church, VA 22042, USA.

[5]The American Genome Center; Uniformed Services University of the Health Sciences, Bethesda, MD 20814, USA

[6]Department of Anatomy Physiology and Genetics, Uniformed Services University, 4301 Jones Bridge Road, Bethesda, MD, 20814 USA.

[7]Institute for Genome Sciences, University of Maryland School of Medicine, Baltimore, MD 21201 USA.

[8]University of California, Davis, One Shields Avenue, Davis, CA 95616 USA.

[9]Chan Soon-Shiong Institute of Molecular Medicine at Windber. Windber, PA 15963 USA.

[10]Wayne State University, Detroit, MI 48202 USA.

[11]Johns Hopkins University Medical Center, Baltimore, MD 21218 USA.

[12]The University of Illinois College of Medicine, Chicago, IL 60612 USA.

[13]Department of Obstetrics and Gynecology, Michigan State University, East, Lansing, MI 48824, USA.

[14]Program in Personalize and Genomic Medicine, University of Maryland School of Medicine, Baltimore, MD 21201 USA.

[15]Marlene and Stewart Greenebaum Comprehensive Cancer, University of Maryland School of Medicine, Baltimore, MD 21201 USA.

*Authors contributed equally to this work.

Keywords: Proteogenomics, Uterine Neoplasms, Ancestry Informative Markers.

Funding Statement: This study was supported in part by the U.S. Department of Defense - Uniformed Services University of the Health Sciences (HU0001-16-2-0006 and HU0001-16-2-0014)

Address correspondence to: Nicholas W. Bateman, PhD. 3289 Woodburn Rd, Suite 375, Annandale, VA, 22003; Tel: 703-207-3362; Email: batemann@whirc.org

Abstract

Characterization of ancestry-linked peptide variants in disease-relevant patient tissues represents a foundational step to connect patient ancestry with molecular disease pathogenesis. Nonsynonymous single nucleotide polymorphisms (SNPs) encoding missense substitutions within tryptic peptides exhibiting high allele frequencies in European, African, and East Asian populations, termed peptide ancestry informative markers (pAIMs), were prioritized from 1000 genomes. *In silico* analysis shows that as few as 20 pAIMs can determine ancestry proportions similarly to >260K SNPs (R^2=0.9905). Multiplexed proteomic analysis of >100 human endometrial cancer cell lines and uterine leiomyoma tissues resulted in the quantitation of 62 pAIMs that correlate with self-described race and genotype-confirmed patient ancestry. Candidates include a D451E substitution in GC vitamin D-binding protein previously associated with altered vitamin D levels in African and European populations. These efforts describe a generalized set of markers for proteoancestry assessment that will further support studies investigating the impact of ancestry on the human proteome and how this relates to the pathogenesis of uterine neoplasms.

Introduction

Proteogenomics aims to integrate protein-level measurements with companion transcriptome and genome sequencing data (1) to elucidate complex systems-level relationships between protein and transcript-level expression including identification of proteins encoding missense substitutions that may impact protein function (1,2). Understanding the impact of proteogenomic alterations on disease risk and patient outcome is a priority for population-level investigations (3), particularly those focusing on cancer, such as efforts by The Cancer Genome Atlas (TCGA) (4) and the recently initiated Applied Proteogenomics OrganizationaL Learning and Outcomes (APOLLO) research network (5). Many historic efforts have poor representation of U.S. minorities amongst patient cohorts analyzed (6) and there remains a paucity of systems-level molecular analyses within powered cohorts to elucidate race-related differences in disease etiology. In the context of gynecologic disease, patients with uterine leiomyomas (fibroids) and endometrial cancers experience significant racial disparities in disease incidence and outcome (7-13). Among possible molecular mechanisms that may give rise to racial disparities in gynecologic disease, one such manifestation could be from non-synonymous single nucleotide polymorphisms (nsSNPs) encoding missense substitutions that may alter protein function(s). Defining ancestry-linked peptide variants in disease-relevant cells and tissues will augment proteogenomic discovery efforts that aim to define molecular drivers underlying racial disparities in gynecologic diseases.

Ancestry informative markers (AIMs) comprise SNPs that are highly differentiated within discrete ancestral populations (14-16). Most of these markers occur within non-protein coding regions, but with large-scale sequencing now available for a diversity of ancestries (17,18), especially in protein coding regions (19,20), it is now possible to assess AIMs that are detectable through proteomics data alone. To this end, efforts to date have identified genetically variant peptides

differentiating individuals of European and African descent (21) as well as Asian populations (22) and these have been explored for forensic human identification, such as through proteomic analyses of human hair and bone samples. We leveraged population-level genotyping data from the 1000 Genomes Project (23) to identify SNPs encoding missense substitutions that exhibit altered allele frequencies with European, African, and East Asian ancestries and prioritized candidates occurring within tryptic peptides observable by routine, bottom-up proteomic workflows to explore these within disease-relevant models and tissues from uterine neoplasms. Although these candidates are not tissue dependent and represent a generalized set of markers for proteoancestry assessment in diverse tissues and cell lines, we show here the ability to ancestrally characterize endometrial cancer cell line models as well as uterine fibroid tissues from women representing diverse racial and ancestral backgrounds using multiplexed proteomic approaches. Our study further defines a foundational set of ancestry-linked variant peptides within uterine tissues that will support ongoing efforts to investigate germline as well as somatic proteogenomic alterations underlying ancestry-linked disease biology and how this may further relate to racial disparities in the pathogenesis of uterine neoplasms.

Results

Selection and *In Silico* Analyses of Peptide Ancestry Informative Markers (pAIMs).

We selected >640K SNPs from the 1000 Genomes Project (23) encoding nonsynonymous substitutions and further filtered them to those exhibiting ≥ 50% allele frequency differences between individuals of European (i.e. FIN, GBR, IBS, and TSI; N=404), African (i.e. ESN, GWD, LWK, MSL, and YRI; N=504), and East Asian (i.e. CDX, CHB, CHS, and KHV; N=400) descent. Candidates were also filtered to prioritize missense substitutions occurring in tryptic peptides (≥6 and ≤40 amino acids in length) that would be observable within “bottom-up”, multiplexed analyses

of disease-relevant cell lines and tissues collected from individuals representing diverse ancestries (Workflow Figure 1A, Supplemental Table 1A). This filtering approach resulted in 1,037 peptide ancestry informative markers (pAIM) mapping to 831 unique proteins spanning all 22 autosomes and exhibit the greatest frequencies on Chr1 (12.3%) and Chr19 (7.5%) (Supplemental Table 1A). Most of these parent proteins encode a single pAIM (Supplemental Table 1A) with a subset of 136 candidates encoding ≥2 pAIMs as well as 3 candidates encoding >5 pAIMs; filaggrin (10 pAIMs), cardiomyopathy-associated protein 5 (7 pAIMs) and HLA class II histocompatibility antigen, DP alpha 1 chain precursor (6 pAIMs). Functional enrichment analyses of proteins encoding pAIMs revealed significant enrichment of cellular pathways regulating the cellular matrisome as well as keratinocyte differentiation and sensory perception (Supplemental Table 1B). Unique pAIMs exhibiting ≥50% allele frequencies were most prevalent in African populations (344 total sites) followed by East Asian (229) and European (79) ancestries and East Asian as well as European populations exhibited nearly 2-fold greater conservation (208) of shared pAIMs relative to African populations (92 and 85 respectively) (Figure 1B). Fixation index (Fst) values for nonsynonymous single nucleotide polymorphisms (SNPs) encoding pAIMs exhibited an average of 0.312 ± 0.1 consistent with Fst threshold expectations for identity-informative SNPs used in forensic DNA sequencing (24) (Supplemental Table 1A). The clinical significance and known disease pathogenicity of SNPs encoding pAIMs within the ClinVar resource was assessed for 1,031 subset pAIMs mapping to the Ensemble Variant Effect Predictor tool (25). Most of these pAIMs had no previous associations with clinical significance. We did however identify 87 pAIMs of unknown clinical significance that map to putative functional protein domains (Figure 2A, Supplemental Table 1A). The remaining candidates were largely undocumented for disease association in ClinVar with seven pAIMs candidates correlating with altered drug responses or as being risk

factors for disease. This latter subset included a substitution in kinesin family member 6 that is associated with altered response to statin treatment (26) (W719R, rs20455) and has higher allele frequencies within African (86%) and East Asian (53%) populations, or as being risk factors for several diseases (Supplemental Table 1A). Risk factors included a substitution in aurora kinase A (F31I, rs2273535) which has higher allele frequencies within East Asians (67%) and is associated with an increased risk of developing colon cancer within these populations (27). We also assessed the impact of pAIM substitutions on protein function via *in silico* prediction analyses using SIFT (28), Poly-Phen-2 (29), and PROVEAN (30) and identified 23 pAIMs that may be deleterious (Figure 2B). Although many of these candidates have unknown clinical significance, five candidates have been shown to not be pathogenic for disease, i.e. categorized by ClinVar as benign or likely benign (Figure 2C, Supplemental Table 1A). These candidates include a substitution in ATP-binding cassette transporter sub-family C member 11 (G180R, rs17822931) that has high allele frequencies within East Asian populations (75%) and is significantly correlated with Axillary Osmidrosis in Chinese Han populations (31) as well as increased risk for breast cancer in Japanese women (32). Further analyses of these 23 putatively deleterious pAIMs revealed they exhibit higher allele frequencies in East Asian versus European and African populations (Figure 2D). We also utilized as a test set of populations CEU, a European population from Utah; ASW, an admixed African-American population from the South West; ACB, an admixed African Caribbean population; and JPT, a Japanese population from East Asia to assess the accuracy of pAIMs to classify ancestral proportions relative to standard genotype estimates *in silico*. We apply a random sampling analyses of nsSNPs encoding pAIMs and compared them to using 266,403 LD-pruned SNPs by standard estimates approaches. We find that as few as 20 variants can recapitulate genome-wide ancestry proportions, using standard approaches (33-35) (error is

increased due to smaller feature set, but average of 500 random sampling assessments remains robust is R^2>0.99) (Figure 3).

Quantitation of Peptide Ancestry Informative Markers (pAIMS) in Endometrial Cancer Cell Lines.

We determined the ancestry of thirteen endometrial cancer cell line models by standard estimates using comparison of whole genome sequencing (WGS) data to reference populations (Table 1). Most EC models were established from women of European descent (n=7), with a subset corresponding to women of African (n=3) and East Asian (n=3) descent. We performed quantitative bottom-up proteomic analyses employing a multiplexed tandem-mass tag (TMT) approach and quantified 133,473 total peptides that included 43 high-confidence pAIM variant peptides (Supplemental Table 2), where MS2 ions flanking the pAIM substitution of interest were confirmed using SpectrumAI (36). Among these pAIMS, 39 were quantified in >50% of all EC cell lines and this feature subset was assessed to investigate pAIM abundance relative to cell line ancestries and genotypes for the nsSNP of interest. Of these pAIM candidates, 30 are of unknown clinical significance, 12 are undocumented for disease association in ClinVar and one candidate (rs8010699) is of uncertain significance for disease. This latter variant encodes a substitution in nesprin-2 (H3309R) that is associated with Emery-Dreifuss muscular dystrophy and has further been correlated with expression of the tumor suppressor cyclin-dependent kinase inhibitor 1 (CDK1/ p21) in HBV-related hepatocellular carcinomas (37). A subset of 17 pAIMs exhibited >50% allele frequency within European ancestry populations and we found that these candidates were significantly elevated in cell lines from individuals of European versus African ancestry (Mann Whitney U (MWU) Median = +1.003 median fold difference, p=0.0333) as well as East Asian ancestry (East Asian ancestry Median = +0.57 median fold difference, p=0.0167)

(Figure 4A). We further find that these European ancestry-correlated pAIMs were most abundant in European ancestry cell lines that were homozygous and heterozygous for the pAIM variant allele (+/+ and -/+ genotype) relative to those homozygous for the reference allele (-/-) (MWU p=0.0006). Another subset of 21 pAIMs quantified exhibited >50% allele frequency within African ancestry populations and were significantly elevated in cell lines from individuals of African versus European (MWU p=0.0333) ancestry and trended as elevated in African versus East Asian ancestry cell lines (+1.0676 median fold difference) (Figure 4B). These African ancestry-associated pAIMs were most abundant in African cell lines homozygous and heterozygous for the pAIM variant allele (+/+ and -/+ genotype) relative to those homozygous for the reference allele (-/-), i.e. +/+ vs. -/- cell lines = +1.69 median fold difference. We also quantified 17 pAIMs exhibiting >50% allele frequency within East Asian populations and found that these are elevated in cell lines from individuals of East Asian versus European ancestry (+0.4058 median fold difference) and African (+0.84563 median fold difference) ancestry (Figure 4C). These East Asian ancestry-related pAIMs further tracked with genotype, i.e. (+/+ pAIM allele versus -/- cell lines = +1.99 median fold difference).

Quantitation of Peptide Ancestry Informative Markers (pAIMS) in Uterine Leiomyoma Tissues.

We assessed pAIMs within multiplexed (TMT) quantitative proteomic analysis of formalin-fixed, paraffin embedded uterine leiomyoma tissues from self-described European-American (n=35) or African-American (n=31) women (Table 2, Discovery). We quantified 69,056 total peptides that included 33 high-confidence pAIMs (Supplemental Table 3). Of these candidates, 24 are of unknown clinical significance while 9 have been reported as not being pathogenic for disease (Supplemental Table 1A, ClinVar). Several of these candidates map to putative functional protein

coding domains including intermediate filament domains within keratin 3 (R375G, >50% AF in Europeans) and keratin 13 (A187V, >90% in Europeans and East Asians) as well as within the dihydroxyacetone- (Dha-)binding domain of DHA kinase (A185T, >90% in Europeans and East Asians) (Supplemental Table 1A). We further assessed the performance of a subset of 18 pAIMs quantified within >50% of all uterine leiomyoma tissues to distinguish patient ancestry stratified by self-described race. Unsupervised hierarchical cluster analyses revealed that the abundance of pAIMs exhibiting high allele frequencies within European or African populations trended with self-described European or African-American race (Figure 5A). We also assessed performance of these candidates using a partial least squares (38) approach and identified, based on principle component analysis, these candidates served to explain 21% and 7% of the variance between African-American and European-American patient tissues (Figure 5B) and can further classify African-American from European-American patients with high accuracy (AUC=0.9834, $P=1.6E^{-11}$, Figure 5C). We also quantified pAIM abundance by multiplexed (TMT), quantitative proteomic analyses within an independent cohort of fresh-frozen uterine leiomyoma tissues from women of European (n=16) or African (n=10) ancestry confirmed using standard genotype estimates from companion WGS analyses, as recently described (39) (Table 2, Validation, Supplemental Table 4). We quantified a total of 61,283 total peptides among which 15 pAIMs were quantified in this cohort and 10 of which were co-quantified with discovery analyses (Supplemental Table 4). This validated subset was predominated by candidates of unknown clinical significance (ClinVar) and included a substitution in GC vitamin D-binding protein, i.e. (D451E, >50% Europeans). Assessment of pAIMs with allele frequencies >50% in African populations were significantly more abundant in African ancestry patients than pAIMS with allele frequencies of >50% in European ancestry populations (+1.0381 median fold difference, MWU p=0.003) (Figure 6A).

Conversely, we find that pAIMs with allele frequencies >50% in European ancestry populations were significantly more abundant in European ancestry patients than pAIMS with allele frequencies >50% in African populations (+1.74 median fold difference, MWU $p<0.0001$ (Figure 6B). Further, as observed in the endometrial cancer cell lines, we find that pAIMs abundances directly correlate with patients homozygous and heterozygous for the pAIM variant allele (+/+ and -/+ genotype) relative to those homozygous for the reference allele (-/-), i.e. African and European ancestry +/+ versus -/- patients ($p<0.0001$).

We further prioritized two pAIMs, i.e. a V237A substitution in protein Serpin Family A Member 1 (SERPINA1, K.DTEEEDFHVDQ(V/A)TTVK) with an allele frequency (AF) = 0.64 in African versus AF = 0.18 in European populations as well as an A19D substitution in Serine/threonine-protein phosphatase CPPED1 (CPPED1, R.TL(A/D)AFPAEK) with an AF = 0.75 in African versus AF = 0.15 in European populations for targeted analysis using a parallel reaction monitoring assay (40). Stable isotope standard (SIS) peptides were synthesized containing heavy isotope-labeled lysine residues and spiked into fibroid FFPE tissue digests collected from a cohort of African-American (n=3) and European-American women (n=3) previously assessed by multiplexed quantitative proteomic analysis (Supplemental Table 3). Quantitation of heavy SIS peptides revealed consistent abundance trends and high dot product similarity scores (dotp) (41) for the top five most abundant y-ions quantified for each peptide relative to library spectra across tissue digests from AA and EA women, i.e. 11.1% CV in abundance and average dotp = 0.92 ± 0.01 for the SERPINA1-V237A variant (Heavy SIS, Figure 7A, Supplemental Table 5) and 10.6% CV in abundance and average dotp = 0.91 ± 0.01 for the CPPED1-A19D variant (Heavy SIS, Figure 7B, Supplemental Table 5). Quantitation of endogenous SERPINA1-V237A and CPPED1-A19D peptides in tissue digests collected from African-American women from revealed high

relative abundances and dot product similarity scores, i.e. SERPINA1-V237A peptide average dotp = 0.94 ± 0.01 (Figure 7A) and CPPED1-A19D peptide average dotp = 0.91 ± 0.03 (Figure 7B). Comparison of heavy SIS and endogenous peptide abundances further showed that SERPINA1-V237A pAIM variant was 6.1 ± 2.46 femtomole (fmol) and CPPED1-A19D variant 0.45 ± 0.12 fmol in fibroid tissue digests collected from African-American women (Table 3). Quantitative assessment of endogenous peptides in tissue digests collected from European-American women revealed peptide variants were largely below signal to noise or not detected and exhibited low dotp scores, i.e. SERPINA1-V237A average dotp = 0.33 ± 0.05 (Figure 7A) and CPPED1-A19D average dotp = 0.1 ± 0.15 (Figure 7B), suggesting these peptides were not present in these patient samples. Endogenous peptide abundance trends observed by targeted analysis are consistent with abundance trends quantified by multiplexed proteomic analysis for these patient tissue samples (Supplemental Table 3).

Discussion

Comprehensive analysis of proteogenomic alterations correlating with patient ancestry are necessary to better understand the relationship between racial disparities underlying disease pathogenesis. In gynecologic malignancies, uterine neoplasms exhibit significant racial disparities, specifically increased incidence of uterine leiomyomas (42) as well as more aggressive endometrial cancers in African-American versus European-American patients (8,43,44). We and others have described race-specific molecular alterations correlating with disease outcome in endometrial cancers (45-47). As a foundational step to support our ongoing investigations of molecular alterations underlying racial disparities in gynecologic malignancies, we have investigated 1,037 nsSNPs exhibiting high allele frequencies within individuals of European, African, and East Asian populations that encode missense substitutions occurring within putative

tryptic peptides, i.e. termed peptide ancestry informative markers (pAIMS) in cell line models and tissues derived from uterine neoplasms collected from women representing diverse ancestral backgrounds. Candidates prioritized were investigated *in silico* for their associations with disease as well as prevalence within putative functional protein domains and for predicted impact on protein function. We found that many pAIMs encode substitutions of unknown clinical significance (ClinVar), occur within functional protein domains and include subsets that are predicted to be deleterious to protein function. We further find that several pAIM variants are linked to an increased risk to develop cancer, such as the F31I substitution in aurora kinase A associated with colon cancer development in East Asian populations (16) and candidates that further track with cancer cell signaling, such as a substitution in nesprin-2 (SYNE2, H3309, rs8010699) that correlates with expression of cyclin-dependent kinase inhibitor 1 (CDK1/ p21) in HBV-related hepatocellular carcinomas (37). We also find that several candidates of unknown clinical significance occur within known functional protein domains including multiple immunoglobulin-like domains, such as in the major histocompatibility complex, class II, DP alpha 1 (HLA-DPA1) protein. These candidates further represent ancestrally-linked, variant peptides theoretically observable with routine LC-MS proteomic workflows encoding substitutions that may alter functional protein domain interactions as well as protein complex architecture.

Our efforts have quantified and validated pAIMs in uterine neoplasms from >100 women representing diverse ancestries and consist of a foundational set of ancestry-linked variant peptides observable by multiplexed proteomic analyses of uterine cells and tissues. Many pAIMs quantified are of unknown clinical significance in ClinVar and may warrant further investigation to better understand possible functional roles in the pathogenesis of uterine disease. Validated candidates were largely undocumented for disease pathogenesis in ClinVar but were associated with altered

biological functions. One such candidate encodes a substitution in GC vitamin D-binding protein, i.e. (D451E, rs7041), a protein that is important in regulating transport of vitamin D, exhibiting a higher allele frequency within individuals of European (58%) versus African (7.3%) descent. rs7041 has been shown to correlate with altered levels of GC within European and African-Americans (48) and further to impact vitamin D metabolism in pregnant women (49). Comparison of cell line and tissue analyses revealed quantitation of pAIMs encoded within Protein-L-isoaspartate(D-aspartate) O-methyltransferase (V178I, >80% AF in African and East Asians), Serine/threonine-protein phosphatase CPPED1 (A19D, >75% AF in Africans) and AH receptor-interacting protein (Q228K, >99% AF in European and East Asians) across all samples. Protein-L-isoaspartate(D-aspartate) O-methyltransferase (PCMT1) regulates methyl esterification of L-isoaspartyl and D-aspartyl residues and has been shown to repair damage to aspartate resides that can occur in an age-dependent manner (50). Interestingly, the I178 variant of PCMT1 has been shown to result in increased catalytic activity and a more thermostable version of PCMT1, while the V178 variants exhibits greater substrate affinity. Serine/threonine-protein phosphatase CPPED1 has been shown to function as a tumor suppressor in bladder cancer via inactivation of Protein Kinase B (AKT) through dephosphorylation of S473 leading to inhibition of cell cycle progression and promotion of apoptosis (51). Although the A19D ancestry-linked substitution we have observed is not predicted to impact CPPED1 function, we have previously reported higher mutational frequencies in the gene encoding tumor suppressor phosphatase and tensin homolog (PTEN) in European-American versus African-American endometrial cancer patients, a regulator of AKT signaling, that correlates with improved outcome in European-American women (46). This intersection suggests that regulation of AKT signaling associated protein machinery may be

linked to patient ancestry and warrants further investigation of these relationships and their impact on disease pathogenesis.

Our analyses provide proof of concept that estimates of European, African and East Asian ancestry can be determined by routine proteomic analysis of disease-relevant patient tissues. We find that pAIMs exhibiting higher allele frequencies within European, African or East Asian ancestry individuals are quantified at significantly greater abundances in cell lines and tissue samples derived from individuals of similar self-described ancestry, i.e. European-American or African-American, and further exhibited abundance trends correlating with patient genotype. Our findings also underscore that quantitation of pAIMs is feasible in formalin-fixed, paraffin embedded as well as fresh frozen human tissue samples. These data extend previous efforts showing that genetically variant peptides can provide estimates of global ancestry in human hair and bone and underscore that these estimates can be determined using multiplexed proteomic data similar to that being generated for population-scale proteogenomic studies focused on improving our understanding of cancer. We further show that we can accurately estimate global ancestry by quantifying as few as 20 population-specific pAIMs in comparison with genotype analyses of ~266K genetic markers using standard estimates (R^2>0.99). Although our focus has been to characterize pAIMs in uterine neoplasms, these candidates are not tissue dependent and represent a generalized set of markers for proteoancestry assessment in diverse tissues and cell lines. To that end, comparison of proteins encoding pAIMs with large-scale proteomic analyses of diverse human cell and tissue types (52) suggests that many of these protein targets are ubiquitously expressed across various tissues, including diverse immune cell types (data not shown) and that quantitation of pAIMs in a wide range of biological samples is likely possible. One limitation of this study we further note is that several pAIMs quantified also map to largely predicted proteins (Uniprot.org and noted in

Supplemental Tables 2 thru 4) underscoring the need to further refine pAIMs panels with the goal of prioritizing candidates that estimate patient ancestry with the greatest sensitivity and specificity for a given organ site. To this end, we further provide proof of concept data for the targeted quantitation of two pAIM candidates, i.e. SERPINA1-V237A and CPPED1-A19D that exhibit higher allele frequencies with African versus European populations in fibroid tissue digests from African-American and European-American women. These analyses verified the relative abundance trends observed for these candidates by multiplexed, quantitative proteomic analysis and further showed these candidates exhibited elevated abundance in African-American women, but were largely not detected within European-American women, consistent with the known allele frequencies for these variants in these populations. These findings will support future efforts focused on optimizing tissue-specific, stable isotope-labelled pAIMs panels that can be co-quantified during primary clinical sample analyses.

We have characterized ancestry-linked peptide variants in endometrial cancer cell lines and patient tissues representing a foundational step towards investigating relationships linking patient ancestry with the proteome, genome and disease pathogenesis. To this end, recent investigations have revealed that clinical serum biomarkers can exhibit altered performance directly as a product of differences in patient genetic ancestry, underscoring the need to integrate proteomics with genetic ancestry assessments at the level of investigational analyses such as biomarker discovery (53). Racial disparities in the incidence and outcome of uterine neoplasms persists following adjustments for socioeconomic variables, such as patient access to care (54) and has fueled efforts to define ancestry-linked molecular alterations that may drive these differences. Our ability to discern these relationships will emerge through the assessment of more ancestrally-diverse populations of women suffering from gynecologic disease as well as within disease-relevant *in*

vitro and *in vivo* models. We recently showed that historic cell line models of cancer have been predominantly established from individuals of European ancestry (55), noting that cancers impacted by racial disparities, such as endometrial cancer, often lacked cell line models from non-European individuals. We confirm here three endometrial cancer cell line models, i.e. NCI-EC1, ACI-80 and ACI-181 are derived from women of African ancestry representing *in vitro* models to investigate ancestry-linked disease biology in endometrial cancers. This work will support ongoing efforts focused on linking the proteome and genome with patient ancestry to better understand relationships with disease mechanisms driving racial disparities in the pathogenesis of uterine neoplasms.

Methods

Prioritization and *In Silico* Analyses of Peptide Ancestry Information Markers.

80,855,907 SNPs for European (i.e. FIN, GBR, IBS, and TSI; N=404), African (i.e. ESN, GWD, LWK, MSL, and YRI; N=504), and East Asian (i.e. CDX, CHB, CHS, and KHV; N=400) were downloaded from the 1000 Genomes Project (23). SNPs were further mapped to refSeq version 85 to identify candidate missense variants (646,768 nsSNPs) occurring within putative tryptic peptides ≥6 or <40 amino acids in length that did not encode isoleucine to leucine substitutions and were further filtered for those exhibiting ≥ 50% difference in allele frequency between European, African, and East Asian populations. These substitutions were then mapped to several RefSeq proteome databases to confirm amino acid substitution positions and tryptic specificity resulting in a final subset of 1,037 candidates. nsSNPs encoding pAIMs were mapped to rsIDs using Kaviar (http://db.systemsbiology.net/kaviar/cgi-pub/Kaviar.pl) against hg19 (GRCh37). Candidates were further assessed using the Variant Effect Predictor tool (https://useast.ensembl.org/Homo_sapiens/Tools/VEP) against hg19 (GRCh37) and extracted metadata detailing putative clinical significance, i.e. ClinVar traits and clinical significance, as well as predicted impact on protein function, i.e. SIFT (28) and Poly-Phen-2 (29) and PROVEAN (30) outputs. Candidates were further mapped to the Uniprot resource and amino acid position of pAIM substitutions were correlated with putative functional domains within parent proteins and pAIM substitutions positions mapping with putative domain regions were prioritized for downstream analyses. Functional enrichment analyses was performed using the “express analysis” settings in MetaScape (56). Determination of fixation index for pAIMs. Fixation index (FST) values were calculated using reference and alternative allele frequency data from the 1000 genomes project. The following equation was used; FST = (HT-HS)/HT, where HT is the expected

heterozygosity in the total population and HS is the expected heterozygosity in the subpopulation (57).

Random Sampling Analysis

After the 1037 pAIMs were selected from the 1000 Genomes Project training data, we then performed ADMIXTURE (34) randomly sampling 20 pAIMs without replacement, using the supervised learning version (33) with the training data as fixed for their respective ancestries (K=3 for African, European, and East Asian). Test data also came from the following 1000 Genomes Project populations (23), which were not included in the training: JPT to represent East Asian, CEU to represent European, and both ACB and ASW as admixed African ancestry. This procedure was repeated 500 times with the mean and standard deviation calculated and plotted against the estimates for these same samples from 266,403 SNPs. This larger set of sites was selected in the standard way (58), where they were LD pruned (using the PLINK(59) command --indep-pairwise 50 5 0.1), and filtered for allele frequency of 5%.

Sample Prep for Proteomics

Cell Lines – Commercial endometrial cancer cell lines, i.e. MFE-296 cells were purchased from DSMZ GmbH (Berlin, Germany) and cultured in MEM with 10% fetal bovine serum (FBS) and 1X penicillin/streptomycin (Pen/Strep). SNG-M cells were purchased from the JCRB cell bank (Osaka, Japan) and cultured in Ham's F12 median with 10% FBS and 1X Pen/Strep. HEC1A (McCoy's 5a with 10% FBS and 1X Pen/Strep), RL95-2 (DMEM:F12, 0.005 mg/mL insulin, 10% FBS and 1X Pen-Strep), Ishikawa (MEM with 2mM Glutamine, 5% Fetal Bovine Serum (FBS) and 1X Pen/Strep), AN3CA (EMEM with 10% FBS and 1X Pen/Strep) and KLE (DMEM:F12 with 10% FBS and 1X Pen/Strep) cells were from ATCC (Manassas, VA). NCI-EC1, ACI-80, ACI-181, ACI-52, ACI-61 and ACI-68 were obtained from John Risinger at Michigan State

University (East Lansing, MI) and maintained in DMEM:F12 with 10% FBS and 1X Pen/Strep (ATCC). Cell lines were plated at equivalent densities and lysed at ~80% confluency in 1% SDS and 10mM Tris-HCl, pH 7.4. Cell lysates (30 µg) were run approximately one inch into a 4-15% bis-acrylamide gel (Bio-Rad) and processed for in-gel digestion as previously described (60). Peptide extracts were labelled with TMT-11 reagents (Thermo Fisher Scientific) as described below.

Uterine Leiomyoma Tissues (Discovery cohort) – Age-matched, formalin-fixed, paraffin embedded uterine leiomyomas from self-described white and black women were obtained under an institutional-review board approved protocol from Inova Fairfax Hospital (Falls Church, VA). Tissue specimens were hematoxylin and eosin (H&E) stained and evaluated by a pathologist to confirm diagnosis. Thin (10 µm) tissue sections were cut using a cryostat and placed on polyethylene naphthalate membrane slides. After staining with aqueous H&E, laser microdissection (LMD) was used to harvest tumor cells from thin sections.

Uterine Fibroid Tissues (Validation cohort) - Flash-frozen uterine leiomyomas were obtained under an institutional-review board approved protocol from Johns Hopkins Memorial Institute (Baltimore, MD). Tissues were cryopulverized, resuspended in 100 mM triethylammonium bicarbonate (TEAB), and sonicated. Protein was quantified by BCA Protein Assay (Thermo Scientific) and 50 µg of total protein in 100 mM TEAB and 10% acetonitrile was incubated at 99 ºC for 1 h.

Sample digestion, TMT labeling and offline fractionation

Sample digestion, TMT labeling and offline fractionation of tissue samples was performed as recently described (61). Briefly**,** tissues were collected in 20 µL of 100 mM TEAB in MicroTubes (Pressure Biosciences, Inc). Following the addition of 1 µg of SMART Digest Trypsin (Thermo

Scientific) to each sample, MicroTubes were capped with MicroPestles. Pressure-assisted lysis and digestion was performed in a barocycler (2320 EXT, Pressure BioSciences, Inc) by sequentially cycling between 45 kpsi and atmospheric pressure for 60 cycles at 50 ºC. The peptide digests were transferred to 0.5 mL microcentrifuge tubes, vacuum-dried, resuspended in 100 mM TEAB, pH 8.0 and the peptide concentration of each digest was determined using the bicinchoninic acid assay (BCA assay). Forty-fifty micrograms of peptide from each sample, along with a pooled reference sample assembled from equivalent amounts of peptide digests pooled from individual patient samples for individual sample sets, were aliquoted into a final volume of 100 µL of 100 mM TEAB and labeled with tandem-mass tag (TMT) isobaric labels (TMT10 or 11plex™ Isobaric Label Reagent Set, Thermo Fisher Scientific) according to the manufacturer's protocol. Each TMT sample plex was fractionated by basic reversed-phase liquid chromatography (bRPLC) into 96 fractions through development of a linear gradient of acetonitrile (0.69%/min). Concatenated fractions (36 total pooled samples for the endometrial cancer cell lines, FFPE ULMs, 24 total for the frozen ULMs) were generated in a serpentine fashion for global LC-MS/MS analysis.

Quantitative Proteomics - LC-MS/MS Analyses

The TMT sample multiplex bRPLC fractions were resuspended in 100 mM NH_4HCO_3 and analyzed by LC-MS/MS employing a nanoflow LC system (EASY-nLC 1200, Thermo Fisher Scientific) coupled online with an Orbitrap Fusion Lumos MS or Q-Exactive HF-X (Thermo Fisher Scientific). In brief, each fraction (~500 ng total peptide) was loaded on a nanoflow HPLC system fitted with a reversed-phase trap column (Acclaim PepMap100 C18, 20 mm, nanoViper, Thermo Scientific) and a heated (50 °C) reversed-phase analytical column (Acclaim PepMap RSLC C18, 2 µm, 100 Å, 75 µm × 500 mm, nanoViper, Thermo Fisher Scientific) coupled online with the MS. Peptides were eluted by developing a linear gradient of 2% mobile phase B (95%

acetonitrile, 0.1% formic acid) to 32% mobile phase B over 120 min at a constant flow rate of 250 nL/min. For both instrument platforms, the electrospray source capillary voltage and temperature were set at 2.0 kV and 275 °C, respectively. High resolution (R=60,000 at m/z 200) broadband (m/z 400-1600) mass spectra (MS) were acquired, followed by selection of the top 12 most intense molecular ions in each MS scan for high-energy collisional dissociation (HCD). Instrument specific parameters were set as follows for each instrument platform. Orbitrap Fusion Lumos - Full MS: AGC, 5e5; RF Lens, 30%; Max IT, 50ms; Charge State, 2-4; Dynamic Exclusion, 10ppm/20 sec; MS2: AGC, 1e5; Max IT, 120ms; Resolution, 50k; Quadrupole Isolation, 0.8 m/z; Isolation Offset, 0.2 m/z; HCD, 38; First Mass, 100. Q Exactive HF-X - Full MS: AGC, 3e6; RF Lens, 40%; Max IT, 45ms; Charge State, 2-4; Dynamic Exclusion, 10ppm/20 sec; MS2: AGC, 1e5; Max IT, 95ms; Resolution, 45k; Quadrupole Isolation, 1.0 m/z; Isolation Offset, 0.2 m/z; NCE, 34; First Mass, 100; Intensity Threshold, 2e5; TMT Optimization, On.

DNA extraction for endometrial cancer cell lines and uterine fibroid tissue samples

Cells were lysed in SNET Digestion buffer (20 mM Tris, 5 mM EDTA, 400 mM NaCl, 1% w/v SDS) with Proteinase K (Thermo Fisher Scientific, Pittsburgh, PA) overnight at 55 ºC with intermittent shaking. An equal volume of 25:24:1 phenol:chloroform:isoamyl alcohol (Thermo Fisher Scientific, Pittsburgh, PA) was added, mixed by inversion and centrifuged at 21,000 x *g* for 5 min. The supernatant was removed to a new tube, half sample volume of 7.5 M ammonium acetate and one and a half sample volumes of 100% ethanol were added, mixed by inversion and centrifuged at 14,000 x *g* for 10 min. The DNA pellet was washed with 70% ethanol and centrifuged at 14,000 x *g* for 5 min. The supernatant was removed and the pellet was air-dried and resuspended in 50 μL of 10 mM Tris buffer. Tissue scrolls were generated from OCT-embedded fresh-frozen tumors and collected in ATL buffer (Qiagen Sciences LLC, Germantown, MD)

482 followed by storage at -80 ºC until isolation. Samples were normalized to 360 μL ATL buffer, 40
483 μL of Proteinase K was added for lysis and incubated at 56 ºC for 4 h with intermittent shaking.
484 Isolation was performed according to the manufacturer's protocol (DNA Purification from
485 Tissues) using the QiAamp DNA Mini Kit (Qiagen Sciences LLC, Germantown, MD). DNA was
486 eluted after a 10 min incubation with 40 μL of Buffer AE, followed by another 10 min incubation
487 with 160 μL of nuclease-free water (Thermo Fisher Scientific) and reduced to 50 μL using a
488 CentriVap Concentrator (Labconco, Kansas City, MO). Quantity and 260/280 purity reading was
489 established using the Nanodrop 2000 Spectrophotometer (Thermo Fisher Scientific) and Quant-iT
490 PicoGreen dsDNA Assay Kit (Thermo Fisher Scientific) according to manufacturer's protocols
491 using eight standards from 0 to 50 ng/uL. Samples were run in triplicate and measurements were
492 taken on a SpectraMax M4 microplate reader (Molecular Devices, San Jose, CA).

493 **DNA PCR-free library preparation and whole genome sequencing**

494 TruSeq DNA PCR-free Library Preparation Kit (Illumina, San Diego, CA) was performed
495 following manufacturer's instructions. Briefly, genomic DNA (gDNA) was diluted to 20 ng/μL
496 using Resuspension Buffer (RSB, Illumina) and 55 μL were transferred to Covaris microTubes
497 (Covaris, Woburn, MA). The normalized gDNA was then sheared on an LE220 focused-
498 ultrasonication system (Covaris) to achieve target peak of 450 bp with an Average Power of 81.0
499 W (SonoLab settings: duty factor, 18.0%; peak incident power, 45.0 watts; 200 cycles per burst;
500 treatment duration, 60 s; water bath temperature, 5 °C – 8.5 °C). The quality of the final DNA
501 libraries was assessed with the High Sensitivity dsDNA (AATI). Per manufacturer's protocol,
502 library peak size was in the range of 550 to 620 bp. The DNA libraries were quantified by real-
503 time quantitative PCR, using the KAPA SYBR FAST Library Quantification Kit (KAPA
504 Biosystems, Boston, MA) optimized for the Roche LightCycler 480 instrument (Roche). DNA

libraries were then normalized to 2 nM and clustered on the Illumina cBot 2 at 200pM using a HiSeq X Flowcell v2 and the HiSeq X HD Paired-End Cluster Generation Kit v2. Paired-end sequencing was performed with the HiSeq X HD SBS Kit (300 cycles) on the Illumina HiSeq X.

Data Processing – Proteomics

Peptide ancestry informative marker identifications are generated by searching .RAW data files with a publicly-available human proteome database (RefSeq human proteome, downloaded 9/22/17 and updated with entries from 8/19/2019 when pAIM amino acid positions did not map to entries in 9/22/17 version) appended with 1,037 full-length proteins encoding predicted pAIM substitutions of interested using Mascot (v2.6.0, Matrix Science) and Proteome Discoverer (v2.2.0.388, Thermo Fisher Scientific) as previously described (61). Samples are searched using the following parameters: precursor mass tolerance of 10 ppm, fragment ion tolerance of 0.05 Da, a maximum of two tryptic miscleavages, dynamic modifications for oxidation (15.9949 Da) on methionine residues and TMT reporter ion tags (229.1629 Da) on peptide N-termini and lysine residues. Peptide spectral matches (PSMs) are filtered using a false-discovery rate (FDR) < 1.0% (Percolator q-value < 0.01). TMT reporter ion intensities are extracted at a mass tolerance of 20 ppm and PSMs lacking TMT reporter ion signal in the pooled reference channel, in all patient TMT channels or exhibiting an isolation interference of ≥50% were excluded from downstream analyses. Normalized peptide abundance was determined by calculating TMT reporter ion ratios relative to a pooled reference channel and applying a mode centered, z-score transformation of each sample channel per TMT multiplex, i.e. normalized (PSM (Log_2Ratio) = (PSM (Log_2Ratio) – ModeCenter (PSM (Log_2Ratio) / σ (PSM (Log_2Ratio). Peptide fragment ion spectra for pAIM peptide variants are confirmed to encode the substitution of interest by automated inspection of MS2 fragment ion spectra in .mzML converted .RAW files (MSConvert, Proteowizard) using

SpectrumAI (36) and the following settings, fragment ion tolerance was set to 50 ppm, relative set to True and a candidate was considered high-confidence if diagnostic ions flanking the substitution of interest were identified in at least one sample multiplex in endometrial cancer cell line and uterine leiomyoma cohorts. Differential analyses of pAIM abundance was performed using Mann-Whitney U rank sum testing in MedCalc (version 19.0.3). pAIMs variants were visualized in heatmaps and by principle component analysis (PCA) using default settings in the ClustVis web tool (https://biit.cs.ut.ee/clustvis/). Sparse Partial Least Squares Discriminant analysis (sPLS-DA) (38) was performed using mixOmics (ver 6.8.5) in RStudio (ver 3.6.0). The sPLS-DA model was run in regression mode for an optimized 18 feature set for two principal components. Plot loadings were calculated using the median to assess contribution onto the first principal component. The AUC and ROC curve were generated from the sPLS-DA model.

Parallel reaction monitoring analysis of SERPINA1-V237A and CPPED1-A19D pAIM candidates

Stable isotope standard versions of SERPINA1-V237A (DTEEEDFHVDQ(A)TTVK) and CPPED1-A19D (TL(D)AFPAEK) pAIM peptide candidates were synthesized with heavy isotope labelled lysine (K, i.e. C13(6), 15N(2) residues (Heavy SIS peptides, Thermo Fisher Scientific). A total of 10fmol final of heavy SIS peptides was spiked into ~1 ug total fibroid tissue digest for each patient sample and samples were analyzed in triplicate by LC-MS/MS employing a nanoflow LC system (EASY-nLC 1200, Thermo Fisher Scientific) coupled online with a Q-Exactive HF-X (Thermo Fisher Scientific). Briefly, each sample was loaded on a nanoflow HPLC system fitted with a reversed-phase trap column (Acclaim PepMap100 C18, 20 mm, nanoViper, Thermo Scientific) and a heated (50 °C) reversed-phase analytical column (Acclaim PepMap RSLC C18, 2 µm, 100 Å, 75 µm × 150 mm, nanoViper, Thermo Scientific) coupled online with the MS.

Peptides were eluted by developing a linear gradient of 2% mobile phase B (95% acetonitrile, 0.1% formic acid) to 32% mobile phase B over 60 min at a constant flow rate of 300 nL/min, then to 99% mobile phase B over an additional 15 min, followed by flushing and re-equilibration prior to the next injection. Source capillary voltage and temperature were set at 2.0 kV and 275 °C, respectively. High resolution (R=120,000 at m/z 200) broadband (m/z 400-1400) mass spectra (MS) were acquired in profile mode, followed by selection of the top 12 most intense molecular ions in each MS scan for high-energy collisional dissociation (HCD). Instrument specific global parameters were set as follows: Full MS: AGC, 3e6; RF Lens, 40%; Max IT, 50 ms; Charge State, 2-3; MS2: AGC, 1e5; Max IT, 50 ms; Resolution, 15k; Quadrupole Isolation, 1.0 m/z; Isolation Offset, 0.2 m/z; NCE, 30; Intensity Threshold, 1.6e5; Dynamic Exclusion, Off; TMT Optimization: Off. Inclusion list entries consisted of the endogenous/variant and heavy/variant SIS pAIMs peptides and the top 12 most abundance molecular ions were selected for data-dependent acquisition when not monitoring inclusion list masses. All targeted peptides were fragmented at an NCE of 28. RAW data files were searched using parameters noted above excluding static modifications for TMT reporter ion tags. RAW data files and Proteome Discoverer search results were imported into Skyline-daily (64-bit, v. 21.0.9.118) (62) using the "Import PRM Peptide Search" workflow and the top five y-ions quantified for heavy stable isotope standard (SIS) and endogenous versions of the SERPINA1-V237A (z = 3+) and CPPED1-A19D (z = 2+) pAIM peptide candidates were extracted using default settings for orbitrap instrumentation. Sum y-ion intensities and dot product similarity scores were exported from Skyline and plotted using Graphpad Prism (v 8.4.3).

DNA WGS processing and variant calling

WGS sample raw reads were aligned to the hg19 reference genome and further processed through the Resequencing workflow within Illumina's HiSeq Analysis Software (HAS; Isis version 2.5.55.1311; https://support.illumina.com/sequencing/sequencing_software/hiseq-analysis-software-v2-1.html). This workflow utilizes the Isaac read aligner (iSAAC-SAAC00776.15.01.27) and variant caller (starka-2.1.4.2) (63), the Manta structural variant caller (version 0.23.1) (64), and the Canvas CNV caller (version 1.1.0.5) (65).).

Global ancestry proportion of EC cell lines

To estimate admixture proportions, we used reference samples with known ancestry from the 1000 Genome Project (23). These reference samples were comprised of 99 European samples from the CEU population, 108 African samples from the YRI population, and 208 Asian samples from the CHB and JPT populations (414 total references samples). Working with genotype data from these reference samples and each of the endometrial cancer cell lines, we first used bcftools(66) to remove Indels and non-biallelic variants. We then used Plink v1.90b3.32 (59)to remove singleton sites (i.e. variants with only one alt allele copy in the dataset. After this processing, we merged these datasets with Plink by taking the intersect of autosomal variants and removing any ambiguous A/T and G/C variants from this combined data. We then pruned for linkage using the plink linkage pruning algorithm command of --indep-pairwise 50 5 0.5, which uses a window of 50 with an r^2 greater than 0.5 and a SNP step of 5. Ancestry was estimated for each cell line independently, and so this process was repeated independently for each cell line. At the end of this processing, we were left with ~500,000 LD-pruned variants per reference cell line merged dataset (range 459,592 – 701,192).

Global ancestry proportion of uterine fibroid patients

We predicted sample super population ancestries using the methods implemented in Peddy (67). Briefly, principal component reduction was performed on genotype calls at specific loci from 2,504 samples in the 1000 Genomes project and a support vector machine (SVM) classifier was trained on the resulting first four components, using known ancestries as the training labels. Genotype calls at the same loci from each sample collected in this study were then mapped to principal component space and the trained SVM was used to predict ancestries. All classifier prediction probabilities were >0.89.

Data Availability: Supplemental data tables include chromosomal loci, missense substitutions and amino acid position, reference SNP Ids (rsIDs) corresponding to peptide ancestry informative markers (pAIMs), as well as pAIM abundances quantified in endometrial cancer cell lines and uterine leiomyoma tissues. RAW LC-MS data files will be deposited in ProteomeXchange.

Acknowledgments: The authors would like to thank Tracy Litzi, BS, Glenn Gist, BS, Julie Oliver, MS, Dave Mitchell, MS, Domenic Tommarello, MS and Wei Ao, BS for their technical contributions as well as Albert Dobi, PhD, Gyorgi Petrovics, PhD and Sara Scannell, BS for critical review of this manuscript. GLM is a consultant for Kiyatec, GSK, and Merck. TPC is a ThermoFisher Scientific, Inc SAB member and receives research funding from AbbVie. GJP has received a patent based on concepts presented in this study, (US 8,877,455 B2, Australian Patent 2011229918, Canadian Patent CA 2794248, and European Patent EP11759843.3). Disclaimer: The views expressed herein are those of the authors and do not reflect the official policy of the Department of Army/Navy/Air Force, Department of Defense, or U.S. Government.

Author Contributions: Contributed to conception: NWB, TDO, TPC, GLM. Contributed to experimental design: NWB, TDO, TPC. Contributed to data acquisition, analysis and/or interpretation of data: NWB, TDO, CMT, TA, BLH, KC, MZ, PT, ARS, AJ, ZG, JL, CT, CD,

MW. Drafted and/or revised the article: NWB, TDO, ARS, MK, CDS, HH, MC, GJP, JS, AAH, JRR, KD, YC, TPC, GLM. Acquired funding for the research: YC, GLM. All authors read and approved the final manuscript.

References

1. Gupta, N., Tanner, S., Jaitly, N., Adkins, J. N., Lipton, M., Edwards, R., Romine, M., Osterman, A., Bafna, V., Smith, R. D., and Pevzner, P. A. (2007) Whole proteome analysis of post-translational modifications: applications of mass-spectrometry for proteogenomic annotation. *Genome Res* **17**, 1362-1377
2. Ng, P. C., and Henikoff, S. (2003) SIFT: Predicting amino acid changes that affect protein function. *Nucleic Acids Res* **31**, 3812-3814
3. Suhre, K., McCarthy, M. I., and Schwenk, J. M. (2020) Genetics meets proteomics: perspectives for large population-based studies. *Nat Rev Genet*
4. Mertins, P., Mani, D. R., Ruggles, K. V., Gillette, M. A., Clauser, K. R., Wang, P., Wang, X., Qiao, J. W., Cao, S., Petralia, F., Kawaler, E., Mundt, F., Krug, K., Tu, Z., Lei, J. T., Gatza, M. L., Wilkerson, M., Perou, C. M., Yellapantula, V., Huang, K. L., Lin, C., McLellan, M. D., Yan, P., Davies, S. R., Townsend, R. R., Skates, S. J., Wang, J., Zhang, B., Kinsinger, C. R., Mesri, M., Rodriguez, H., Ding, L., Paulovich, A. G., Fenyo, D., Ellis, M. J., Carr, S. A., and Nci, C. (2016) Proteogenomics connects somatic mutations to signalling in breast cancer. *Nature* **534**, 55-62
5. Fiore, L. D., Rodriguez, H., and Shriver, C. D. (2017) Collaboration to Accelerate Proteogenomics Cancer Care: The Department of Veterans Affairs, Department of Defense, and the National Cancer Institute's Applied Proteogenomics OrganizationaL Learning and Outcomes (APOLLO) Network. *Clin Pharmacol Ther* **101**, 619-621
6. Spratt, D. E., Chan, T., Waldron, L., Speers, C., Feng, F. Y., Ogunwobi, O. O., and Osborne, J. R. (2016) Racial/Ethnic Disparities in Genomic Sequencing. *JAMA Oncol* **2**, 1070-1074
7. Deshmukh, S. K., Azim, S., Ahmad, A., Zubair, H., Tyagi, N., Srivastava, S. K., Bhardwaj, A., Singh, S., Rocconi, R. P., and Singh, A. P. (2017) Biological basis of cancer health disparities: resources and challenges for research. *Am J Cancer Res* **7**, 1-12
8. Tarney, C. M., Tian, C., Wang, G., Dubil, E. A., Bateman, N. W., Chan, J. K., Elshaikh, M. A., Cote, M. L., Schildkraut, J. M., Shriver, C. D., Conrads, T. P., Hamilton, C. A., Maxwell, G. L., and Darcy, K. M. (2018) Impact of age at diagnosis on racial disparities in endometrial cancer patients. *Gynecol Oncol* **149**, 12-21
9. Felix, A. S., Linkov, F., Maxwell, G. L., Ragin, C., and Taioli, E. (2011) Racial disparities in risk of second primary cancers in endometrial cancer patients: Analysis of SEER Data. *Int J Gynecol Cancer* **21**, 309-315
10. Allard, J. E., and Maxwell, G. L. (2009) Race disparities between black and white women in the incidence, treatment, and prognosis of endometrial cancer. *Cancer Control* **16**, 53-56
11. Farley, J., Risinger, J. I., Rose, G. S., and Maxwell, G. L. (2007) Racial disparities in blacks with gynecologic cancers. *Cancer* **110**, 234-243

12. Maxwell, G. L., Tian, C., Risinger, J., Brown, C. L., Rose, G. S., Thigpen, J. T., Fleming, G. F., Gallion, H. H., Brewster, W. R., and Gynecologic Oncology Group, s. (2006) Racial disparity in survival among patients with advanced/recurrent endometrial adenocarcinoma: a Gynecologic Oncology Group study. *Cancer* **107**, 2197-2205
13. Mahdi, H., Schlick, C. J., Kowk, L. L., Moslemi-Kebria, M., and Michener, C. (2014) Endometrial cancer in Asian and American Indian/Alaskan Native women: tumor characteristics, treatment and outcome compared to non-Hispanic white women. *Gynecol Oncol* **132**, 443-449
14. Enoch, M. A., Shen, P. H., Xu, K., Hodgkinson, C., and Goldman, D. (2006) Using ancestry-informative markers to define populations and detect population stratification. *J Psychopharmacol* **20**, 19-26
15. Kosoy, R., Nassir, R., Tian, C., White, P. A., Butler, L. M., Silva, G., Kittles, R., Alarcon-Riquelme, M. E., Gregersen, P. K., Belmont, J. W., De La Vega, F. M., and Seldin, M. F. (2009) Ancestry informative marker sets for determining continental origin and admixture proportions in common populations in America. *Hum Mutat* **30**, 69-78
16. Galanter, J. M., Fernandez-Lopez, J. C., Gignoux, C. R., Barnholtz-Sloan, J., Fernandez-Rozadilla, C., Via, M., Hidalgo-Miranda, A., Contreras, A. V., Figueroa, L. U., Raska, P., Jimenez-Sanchez, G., Zolezzi, I. S., Torres, M., Ponte, C. R., Ruiz, Y., Salas, A., Nguyen, E., Eng, C., Borjas, L., Zabala, W., Barreto, G., Gonzalez, F. R., Ibarra, A., Taboada, P., Porras, L., Moreno, F., Bigham, A., Gutierrez, G., Brutsaert, T., Leon-Velarde, F., Moore, L. G., Vargas, E., Cruz, M., Escobedo, J., Rodriguez-Santana, J., Rodriguez-Cintron, W., Chapela, R., Ford, J. G., Bustamante, C., Seminara, D., Shriver, M., Ziv, E., Burchard, E. G., Haile, R., Parra, E., Carracedo, A., and Consortium, L. (2012) Development of a panel of genome-wide ancestry informative markers to study admixture throughout the Americas. *PLoS Genet* **8**, e1002554
17. Mathias, R. A., Taub, M. A., Gignoux, C. R., Fu, W., Musharoff, S., O'Connor, T. D., Vergara, C., Torgerson, D. G., Pino-Yanes, M., Shringarpure, S. S., Huang, L., Rafaels, N., Boorgula, M. P., Johnston, H. R., Ortega, V. E., Levin, A. M., Song, W., Torres, R., Padhukasahasram, B., Eng, C., Mejia-Mejia, D. A., Ferguson, T., Qin, Z. S., Scott, A. F., Yazdanbakhsh, M., Wilson, J. G., Marrugo, J., Lange, L. A., Kumar, R., Avila, P. C., Williams, L. K., Watson, H., Ware, L. B., Olopade, C., Olopade, O., Oliveira, R., Ober, C., Nicolae, D. L., Meyers, D., Mayorga, A., Knight-Madden, J., Hartert, T., Hansel, N. N., Foreman, M. G., Ford, J. G., Faruque, M. U., Dunston, G. M., Caraballo, L., Burchard, E. G., Bleecker, E., Araujo, M. I., Herrera-Paz, E. F., Gietzen, K., Grus, W. E., Bamshad, M., Bustamante, C. D., Kenny, E. E., Hernandez, R. D., Beaty, T. H., Ruczinski, I., Akey, J., Caapa, and Barnes, K. C. (2016) A continuum of admixture in the Western Hemisphere revealed by the African Diaspora genome. *Nat Commun* **7**, 12522
18. Kessler, M. D., Yerges-Armstrong, L., Taub, M. A., Shetty, A. C., Maloney, K., Jeng, L. J., Ruczinski, I., Levin, A. M., Williams, L. K., Beaty, T. H., Mathias, R. A., Barnes, K. C., Consortium on Asthma among African-ancestry Populations in the, A., and O'Connor, T. D. (2016) Challenges and disparities in the application of personalized genomic medicine to populations with African ancestry. *Nat Commun* **7**, 12521
19. Tennessen, J. A., Bigham, A. W., O'Connor, T. D., Fu, W., Kenny, E. E., Gravel, S., McGee, S., Do, R., Liu, X., Jun, G., Kang, H. M., Jordan, D., Leal, S. M., Gabriel, S., Rieder, M. J., Abecasis, G., Altshuler, D., Nickerson, D. A., Boerwinkle, E., Sunyaev, S., Bustamante, C. D., Bamshad, M. J., Akey, J. M., Broad, G. O., Seattle, G. O., and Project,

N. E. S. (2012) Evolution and functional impact of rare coding variation from deep sequencing of human exomes. *Science* **337**, 64-69

20. Tennessen, J. A., O'Connor, T. D., Bamshad, M. J., and Akey, J. M. (2011) The promise and limitations of population exomics for human evolution studies. *Genome Biol* **12**, 127
21. Parker, G. J., Leppert, T., Anex, D. S., Hilmer, J. K., Matsunami, N., Baird, L., Stevens, J., Parsawar, K., Durbin-Johnson, B. P., Rocke, D. M., Nelson, C., Fairbanks, D. J., Wilson, A. S., Rice, R. H., Woodward, S. R., Bothner, B., Hart, B. R., and Leppert, M. (2016) Demonstration of Protein-Based Human Identification Using the Hair Shaft Proteome. *PLoS One* **11**, e0160653
22. Feng Lei, J. L., Li Shaun-Fei, Zhang Jian, Liu Hai-bo, Ji An-Quan, Ye Jian, Wang Gui-Qiang, Li Cai-Xia. (2019) Development and Validation of Protein-based Forensic Ancestry Inference Method Using Hair Shaft Proteome. *Progress in Biochemistry and Biophysics* **46（1）：81~88**
23. Genomes Project, C., Auton, A., Brooks, L. D., Durbin, R. M., Garrison, E. P., Kang, H. M., Korbel, J. O., Marchini, J. L., McCarthy, S., McVean, G. A., and Abecasis, G. R. (2015) A global reference for human genetic variation. *Nature* **526**, 68-74
24. King, J. L., Churchill, J. D., Novroski, N. M. M., Zeng, X., Warshauer, D. H., Seah, L. H., and Budowle, B. (2018) Increasing the discrimination power of ancestry- and identity-informative SNP loci within the ForenSeq DNA Signature Prep Kit. *Forensic Sci Int Genet* **36**, 60-76
25. McLaren, W., Gil, L., Hunt, S. E., Riat, H. S., Ritchie, G. R., Thormann, A., Flicek, P., and Cunningham, F. (2016) The Ensembl Variant Effect Predictor. *Genome Biol* **17**, 122
26. Ruiz-Iruela, C., Padro-Miquel, A., Pinto-Sala, X., Baena-Diez, N., Caixas-Pedragos, A., Guell-Miro, R., Navarro-Badal, R., Jusmet-Miguel, X., Calmarza, P., Puzo-Foncilla, J. L., Alia-Ramos, P., and Candas-Estebanez, B. (2018) KIF6 gene as a pharmacogenetic marker for lipid-lowering effect in statin treatment. *PLoS One* **13**, e0205430
27. Xu, L., Zhou, X., Jiang, F., Xu, L., and Yin, R. (2014) STK15 rs2273535 polymorphism and cancer risk: a meta-analysis of 74,896 subjects. *Cancer Epidemiol* **38**, 111-117
28. Sim, N. L., Kumar, P., Hu, J., Henikoff, S., Schneider, G., and Ng, P. C. (2012) SIFT web server: predicting effects of amino acid substitutions on proteins. *Nucleic Acids Res* **40**, W452-457
29. Adzhubei, I., Jordan, D. M., and Sunyaev, S. R. (2013) Predicting functional effect of human missense mutations using PolyPhen-2. *Curr Protoc Hum Genet* **Chapter 7**, Unit7 20
30. Choi, Y., Sims, G. E., Murphy, S., Miller, J. R., and Chan, A. P. (2012) Predicting the functional effect of amino acid substitutions and indels. *PLoS One* **7**, e46688
31. Ren, Y., Liu, W., Chen, J., Wang, J., Wang, K., Zhou, J., Cai, S., Zheng, M., Liu, J., Liu, L., and Xue, D. (2017) A missense variant of the ABCC11 gene is associated with Axillary Osmidrosis susceptibility and clinical phenotypes in the Chinese Han Population. *Sci Rep* **7**, 46335
32. Ishiguro, J., Ito, H., Tsukamoto, M., Iwata, H., Nakagawa, H., and Matsuo, K. (2019) A functional single nucleotide polymorphism in ABCC11, rs17822931, is associated with the risk of breast cancer in Japanese. *Carcinogenesis* **40**, 537-543
33. Alexander, D. H., and Lange, K. (2011) Enhancements to the ADMIXTURE algorithm for individual ancestry estimation. *BMC bioinformatics* **12**, 246

34. Alexander, D. H., Novembre, J., and Lange, K. (2009) Fast model-based estimation of ancestry in unrelated individuals. *Genome Res* **19**, 1655-1664
35. Kessler, M. D., Yerges-Armstrong, L., Taub, M. A., Shetty, A. C., Maloney, K., Jeng, L. J., Ruczinski, I., Levin, A. M., Williams, L. K., Beaty, T. H., Mathias, R. A., Barnes, K. C., and O'Connor, T. D. (2016) Challenges and disparities in the application of personalized genomic medicine to populations with African ancestry. *Nat Commun* **7**, 12521
36. Zhu, Y., Orre, L. M., Johansson, H. J., Huss, M., Boekel, J., Vesterlund, M., Fernandez-Woodbridge, A., Branca, R. M. M., and Lehtio, J. (2018) Discovery of coding regions in the human genome by integrated proteogenomics analysis workflow. *Nat Commun* **9**, 903
37. Han, C., Liao, X., Qin, W., Yu, L., Liu, X., Chen, G., Liu, Z., Lu, S., Chen, Z., Su, H., Zhu, G., Lu, Z., Liu, Z., Qin, X., Gui, Y., Mo, Z., Li, L., and Peng, T. (2016) EGFR and SYNE2 are associated with p21 expression and SYNE2 variants predict post-operative clinical outcomes in HBV-related hepatocellular carcinoma. *Sci Rep* **6**, 31237
38. Le Cao, K. A., Boitard, S., and Besse, P. (2011) Sparse PLS discriminant analysis: biologically relevant feature selection and graphical displays for multiclass problems. *BMC Bioinformatics* **12**, 253
39. Bateman, N. W., Tarney, C. M., Abulez, T., Soltis, A. R., Zhou, M., Conrads, K., Litzi, T., Oliver, J., Hood, B., Driggers, P., Viollet, C., Dalgard, C., Wilkerson, M., Catherino, W., Hamilton, C. A., Darcy, K. M., Casablanca, Y., Al-Hendy, A., Segars, J., Conrads, T. P., and Larry Maxwell, G. (2021) Proteogenomic landscape of uterine leiomyomas from hereditary leiomyomatosis and renal cell cancer patients. *Sci Rep* **11**, 9371
40. Peterson, A. C., Russell, J. D., Bailey, D. J., Westphall, M. S., and Coon, J. J. (2012) Parallel reaction monitoring for high resolution and high mass accuracy quantitative, targeted proteomics. *Mol Cell Proteomics* **11**, 1475-1488
41. Schilling, B., Rardin, M. J., MacLean, B. X., Zawadzka, A. M., Frewen, B. E., Cusack, M. P., Sorensen, D. J., Bereman, M. S., Jing, E., Wu, C. C., Verdin, E., Kahn, C. R., Maccoss, M. J., and Gibson, B. W. (2012) Platform-independent and label-free quantitation of proteomic data using MS1 extracted ion chromatograms in skyline: application to protein acetylation and phosphorylation. *Mol Cell Proteomics* **11**, 202-214
42. Baird, D. D., Dunson, D. B., Hill, M. C., Cousins, D., and Schectman, J. M. (2003) High cumulative incidence of uterine leiomyoma in black and white women: ultrasound evidence. *Am J Obstet Gynecol* **188**, 100-107
43. American Cancer Society. (2016) Cancer Facts & Figures for African Americans 2016-2018., American Cancer Society, Atlanta, GA
44. Rocconi, R. P., Lankes, H. A., Brady, W. E., Goodfellow, P. J., Ramirez, N. C., Alvarez, R. D., Creasman, W., and Fernandez, J. R. (2016) The role of racial genetic admixture with endometrial cancer outcomes: An NRG Oncology/Gynecologic Oncology Group study. *Gynecol Oncol* **140**, 264-269
45. Bateman, N. W., Dubil, E. A., Wang, G., Hood, B. L., Oliver, J. M., Litzi, T. A., Gist, G. D., Mitchell, D. A., Blanton, B., Phippen, N. T., Tian, C., Zahn, C. M., Cohn, D. E., Havrilesky, L. J., Berchuck, A., Shriver, C. D., Darcy, K. M., Hamilton, C. A., Conrads, T. P., and Maxwell, G. L. (2017) Race-specific molecular alterations correlate with differential outcomes for black and white endometrioid endometrial cancer patients. *Cancer* **123**, 4004-4012

46. Maxwell, G. L., Risinger, J. I., Hayes, K. A., Alvarez, A. A., Dodge, R. K., Barrett, J. C., and Berchuck, A. (2000) Racial disparity in the frequency of PTEN mutations, but not microsatellite instability, in advanced endometrial cancers. *Clin Cancer Res* **6**, 2999-3005
47. Dubil, E. A., Tian, C., Wang, G., Tarney, C. M., Bateman, N. W., Levine, D. A., Conrads, T. P., Hamilton, C. A., Maxwell, G. L., and Darcy, K. M. (2018) Racial disparities in molecular subtypes of endometrial cancer. *Gynecol Oncol* **149**, 106-116
48. Powe, C. E., Evans, M. K., Wenger, J., Zonderman, A. B., Berg, A. H., Nalls, M., Tamez, H., Zhang, D., Bhan, I., Karumanchi, S. A., Powe, N. R., and Thadhani, R. (2013) Vitamin D-binding protein and vitamin D status of black Americans and white Americans. *N Engl J Med* **369**, 1991-2000
49. Ganz, A. B., Park, H., Malysheva, O. V., and Caudill, M. A. (2018) Vitamin D binding protein rs7041 genotype alters vitamin D metabolism in pregnant women. *FASEB J* **32**, 2012-2020
50. DeVry, C. G., and Clarke, S. (1999) Polymorphic forms of the protein L-isoaspartate (D-aspartate) O-methyltransferase involved in the repair of age-damaged proteins. *J Hum Genet* **44**, 275-288
51. Zhuo, D. X., Zhang, X. W., Jin, B., Zhang, Z., Xie, B. S., Wu, C. L., Gong, K., and Mao, Z. B. (2013) CSTP1, a novel protein phosphatase, blocks cell cycle, promotes cell apoptosis, and suppresses tumor growth of bladder cancer by directly dephosphorylating Akt at Ser473 site. *PLoS One* **8**, e65679
52. Kim, M. S., Pinto, S. M., Getnet, D., Nirujogi, R. S., Manda, S. S., Chaerkady, R., Madugundu, A. K., Kelkar, D. S., Isserlin, R., Jain, S., Thomas, J. K., Muthusamy, B., Leal-Rojas, P., Kumar, P., Sahasrabuddhe, N. A., Balakrishnan, L., Advani, J., George, B., Renuse, S., Selvan, L. D., Patil, A. H., Nanjappa, V., Radhakrishnan, A., Prasad, S., Subbannayya, T., Raju, R., Kumar, M., Sreenivasamurthy, S. K., Marimuthu, A., Sathe, G. J., Chavan, S., Datta, K. K., Subbannayya, Y., Sahu, A., Yelamanchi, S. D., Jayaram, S., Rajagopalan, P., Sharma, J., Murthy, K. R., Syed, N., Goel, R., Khan, A. A., Ahmad, S., Dey, G., Mudgal, K., Chatterjee, A., Huang, T. C., Zhong, J., Wu, X., Shaw, P. G., Freed, D., Zahari, M. S., Mukherjee, K. K., Shankar, S., Mahadevan, A., Lam, H., Mitchell, C. J., Shankar, S. K., Satishchandra, P., Schroeder, J. T., Sirdeshmukh, R., Maitra, A., Leach, S. D., Drake, C. G., Halushka, M. K., Prasad, T. S., Hruban, R. H., Kerr, C. L., Bader, G. D., Iacobuzio-Donahue, C. A., Gowda, H., and Pandey, A. (2014) A draft map of the human proteome. *Nature* **509**, 575-581
53. Sjaarda, J., Gerstein, H. C., Kutalik, Z., Mohammadi-Shemirani, P., Pigeyre, M., Hess, S., and Pare, G. (2020) Influence of Genetic Ancestry on Human Serum Proteome. *Am J Hum Genet* **106**, 303-314
54. Oliver, K. E., Enewold, L. R., Zhu, K., Conrads, T. P., Rose, G. S., Maxwell, G. L., and Farley, J. H. (2011) Racial disparities in histopathologic characteristics of uterine cancer are present in older, not younger blacks in an equal-access environment. *Gynecol Oncol* **123**, 76-81
55. Kessler, M. D., Bateman, N. W., Conrads, T. P., Maxwell, G. L., Dunning Hotopp, J. C., and O'Connor, T. D. (2019) Ancestral characterization of 1018 cancer cell lines highlights disparities and reveals gene expression and mutational differences. *Cancer* **125**, 2076-2088
56. Zhou, Y., Zhou, B., Pache, L., Chang, M., Khodabakhshi, A. H., Tanaseichuk, O., Benner, C., and Chanda, S. K. (2019) Metascape provides a biologist-oriented resource for the analysis of systems-level datasets. *Nat Commun* **10**, 1523

57. Weir, B. S., and Cockerham, C. C. (1984) Estimating F-Statistics for the Analysis of Population Structure. *Evolution* **38**, 1358-1370
58. Kessler, M. D., Yerges-Armstrong, L., Taub, M. A., Shetty, A. C., Maloney, K., Jeng, L. J. B., Ruczinski, I., Levin, A. M., Williams, L. K., Beaty, T. H., Mathias, R. A., Barnes, K. C., Consortium on Asthma among African-ancestry Populations in the, A., and O'Connor, T. D. (2016) Challenges and disparities in the application of personalized genomic medicine to populations with African ancestry. *Nat Commun* **7**, 12521
59. Purcell, S., Neale, B., Todd-Brown, K., Thomas, L., Ferreira, M. A., Bender, D., Maller, J., Sklar, P., de Bakker, P. I., Daly, M. J., and Sham, P. C. (2007) PLINK: a tool set for whole-genome association and population-based linkage analyses. *Am J Hum Genet* **81**, 559-575
60. Bateman, N. W., Jaworski, E., Ao, W., Wang, G., Litzi, T., Dubil, E., Marcus, C., Conrads, K. A., Teng, P. N., Hood, B. L., Phippen, N. T., Vasicek, L. A., McGuire, W. P., Paz, K., Sidransky, D., Hamilton, C. A., Maxwell, G. L., Darcy, K. M., and Conrads, T. P. (2015) Elevated AKAP12 in paclitaxel-resistant serous ovarian cancer cells is prognostic and predictive of poor survival in patients. *J Proteome Res* **14**, 1900-1910
61. Lee, S., Zhao, L., Rojas, C., Bateman, N. W., Yao, H., Lara, O. D., Celestino, J., Morgan, M. B., Nguyen, T. V., Conrads, K. A., Rangel, K. M., Dood, R. L., Hajek, R. A., Fawcett, G. L., Chu, R. A., Wilson, K., Loffredo, J. L., Viollet, C., Jazaeri, A. A., Dalgard, C. L., Mao, X., Song, X., Zhou, M., Hood, B. L., Banskota, N., Wilkerson, M. D., Te, J., Soltis, A. R., Roman, K., Dunn, A., Cordover, D., Eterovic, A. K., Liu, J., Burks, J. K., Baggerly, K. A., Fleming, N. D., Lu, K. H., Westin, S. N., Coleman, R. L., Mills, G. B., Casablanca, Y., Zhang, J., Conrads, T. P., Maxwell, G. L., Futreal, P. A., and Sood, A. K. (2020) Molecular Analysis of Clinically Defined Subsets of High-Grade Serous Ovarian Cancer. *Cell Rep* **31**, 107502
62. MacLean, B., Tomazela, D. M., Shulman, N., Chambers, M., Finney, G. L., Frewen, B., Kern, R., Tabb, D. L., Liebler, D. C., and MacCoss, M. J. (2010) Skyline: an open source document editor for creating and analyzing targeted proteomics experiments. *Bioinformatics* **26**, 966-968
63. Raczy, C., Petrovski, R., Saunders, C. T., Chorny, I., Kruglyak, S., Margulies, E. H., Chuang, H. Y., Kallberg, M., Kumar, S. A., Liao, A., Little, K. M., Stromberg, M. P., and Tanner, S. W. (2013) Isaac: ultra-fast whole-genome secondary analysis on Illumina sequencing platforms. *Bioinformatics* **29**, 2041-2043
64. Chen, X., Schulz-Trieglaff, O., Shaw, R., Barnes, B., Schlesinger, F., Kallberg, M., Cox, A. J., Kruglyak, S., and Saunders, C. T. (2016) Manta: rapid detection of structural variants and indels for germline and cancer sequencing applications. *Bioinformatics* **32**, 1220-1222
65. Roller, E., Ivakhno, S., Lee, S., Royce, T., and Tanner, S. (2016) Canvas: versatile and scalable detection of copy number variants. *Bioinformatics* **32**, 2375-2377
66. Narasimhan, V., Danecek, P., Scally, A., Xue, Y., Tyler-Smith, C., and Durbin, R. (2016) BCFtools/RoH: a hidden Markov model approach for detecting autozygosity from next-generation sequencing data. *Bioinformatics* **32**, 1749-1751
67. Pedersen, B. S., and Quinlan, A. R. (2017) Who's Who? Detecting and Resolving Sample Anomalies in Human DNA Sequencing Studies with Peddy. *Am J Hum Genet* **100**, 406-413

Tables

Table 1: Endometrial Cancer Cell Lines Analyzed by Whole Genome Sequence and Quantitative Proteomic Analyses. Cell lines include both primary and commercial cell lines and global ancestry was determined by standard estimates using single nucleotide variant-derived ancestry informative markers measured by whole genome sequence analyses.

Cell line	Histology	Ancestry (Standard Estimate)
ACI181	Endometrioid	African
ACI80	Endometrioid	African
NCIEC1	Endometrioid	African
HEC1A	Adenocarcinoma NOS	East Asian
ISHIKAWA	Adenocarcinoma NOS	East Asian
SNGM	Adenocarcinoma NOS	East Asian
ACI52	Endometrioid	European
ACI61	Endometrioid	European
ACI68	Endometrioid	European
AN3CA	Adenocarcinoma NOS	European
KLE	Adenocarcinoma NOS	European
MFE296	Adenocarcinoma NOS	European
RL952	Adenocarcinoma NOS	European

Table 2: Uterine Leiomyoma (ULM) Tissues Analyzed by Quantitative Proteomic (Discovery and Validation) as well as Whole Genome Sequencing (Validation) Analysis. Global ancestry was determined by standard estimates for the validation cohort using single nucleotide variant-derived ancestry informative markers measured by whole genome sequence analyses.

Discovery - ULM Tissues (n=66)	
Ancestry (Self-Described)	**#**
European-American	35
African-American	31

Validation - ULM Tissues (n=26)	
Ancestry (Standard Estimate)	**#**
European	16
African	10

Table 3: Targeted quantitation of SERPINA1-V237A and CPPED1-A19D stable isotope standard and endogenous pAIM peptide candidates in uterine fibroid tissue digests from African-American (AA) patients. fmol = femtomole

Patient ID & Self-Described Race	SERPINA1 - V237A Endogenous/Heavy SIS Peptide Ratio	SERPINA1 - V237A Endogenous Peptide Abundance (fmol)	CPPED1 – A19D Endogenous/Heavy SIS Peptide Ratio	CPPED1 – A19D Endogenous Peptide Abundance (fmol)
Patient 25_AA	0.88	8.8	0.054	0.54
Patient 48_AA	0.54	5.4	0.03	0.3
Patient 54_AA	0.4	4.0	0.05	0.5

Figure Legends

Figure 1: Selection of Peptide Ancestry Informative Markers (pAIMs) and Workflow for Analyses in Cell Lines Models and Tissues of Uterine Neoplasms collected from Women of Diverse Ancestries. A: >640K single nucleotide polymorphisms (SNPs) were filtered to prioritize 1,037 missense substitutions occurring within lysine or arginine-terminating tryptic peptides, ≥ 6 and ≤ 40 amino acids in length, "so-called" peptide ancestry informative markers (pAIMs). We then investigated pAIMs in endometrial cancer cell line models as well as uterine leiomyoma tissues from women representing diverse ancestries. B: Comparison of pAIMs exhibiting ≥ 50% allele frequencies within individuals of European (EUR), African (AFR) or East Asian (EAS).

Figure 2: *In silico* analyses of Peptide Ancestry Informative Markers (pAIMs) to assess Clinical Significance, Localization to Protein Domains as well as to Predict Impact on Protein Function. A: Clinical significance (ClinVar) and protein domain (Uniprot) localization of 1,037 pAIMs. B: Comparison of pAIMs predicted to be deleterious to protein function by PROVEAN, PolyPhen and SIFT functional prediction tools. C: Clinical significance (ClinVar) and protein domain (Uniprot) localization of pAIMs predicted to be deleterious to protein function. D: Allele frequency of pAIMs predicted to be deleterious to protein function in European (EUR), African (AFR) or East Asian (EAS) populations

Figure 3: Comparison of European (EUR), African (AFR) or East Asian (EAS) Global Ancestry Classification using Peptide Ancestry Informative Markers (pAIMs) with Standard Estimates. Random sampling of pAIMs in European, African and East Asian reference populations from 1K genome project revealed that a minimum of 20 pAIM-encoding

nonsynonymous single nucleotide polymorphisms (SNPs) can classify global ancestry with accuracy comparable to standard estimates using >266,000 SNPs, i.e. R^2=0.9943 ± 0.005.

Figure 4: Quantitation of Peptide Ancestry Informative Markers (pAIMs) within Endometrial cancer cell Lines. A: Box plots detail the median logFC abundance of 17 EUR pAIMs within cell lines stratified by European (EUR), African (AFR) or East Asian (EAS) ancestry as well as by pAIM variant allele genotype observed by companion whole genome sequence analyses of EUR cell lines. B: Box plots details the median logFC abundance of 21 AFR pAIMs within cell lines stratified by European (EUR), African (AFR) or East Asian (EAS) ancestry as well as by as well as by pAIM variant allele genotype observed by companion whole genome sequence analyses of AFR cell lines. C: Box plots detail the median logFC abundance of 17 EAS pAIMs within cell lines stratified by European (EUR), African (AFR) or East Asian (EAS) ancestry as well as by pAIM variant allele genotype observed by companion whole genome sequence analyses of EAS cell lines.

Figure 5: Quantitation of Peptide Ancestry Informative Markers (pAIMs) within Uterine Leiomyoma (ULM) Tissues Collected from a Cohort of Women of Self-Described Black or White Race. A: Data reflects unsupervised cluster analyses of 18 pAIMs quantified across n66 patient tissue samples; heatmap reflects clustering by Euclidean distance and complete linkage. B: Principle component analyses of 18 pAIMs, principal component 1 and principal component 2 that explain 21% and 7% of the total variance, respectively. C: Receiver operator curve assessing the performance of 18 pAIMs to classify African-American (n31) versus European-American (n35) patients.

Figure 6: Validation of Peptide Ancestry Informative Markers (pAIMs) within Uterine Leiomyoma (ULM) Tissues Collected from Women with Global Ancestry determined by Standard Estimates. A: Box plots details the median logFC abundance for pAIMs exhibiting >50% allele frequencies in African (8 of 15 pAIMs quantified) reference populations across n10 ULMs sample from women with AFR ancestry as well as by pAIM variant allele genotype observed by companion whole genome sequence analyses. B: Box plots details the median logFC abundance pAIMs exhibiting >50% allele frequencies for European (5 of 15 quantified) reference populations quantified across n=16 ULMs sample from women with EUR ancestry as well as by pAIM variant allele genotype observed by companion whole genome sequence analyses.

Figure 7: Targeted Quantitation of SERPINA1-V237A and CPPED1-A19D pAIM Candidates in Fibroid Tissue Digests from African-American and European-American Women. Stable isotope standard (SIS) peptides were synthesized with heavy-isotope labelled lysine residues corresponding to SERPINA1-V237A pAIM (K.DTEEEDFHVDQ(A)TTVK) and CPPED1-A19D (R.TL(D)AFPAEK) pAIM candidates and heavy SIS and endogenous peptide abundances were assessed by parallel reaction monitoring assay in fibroid FFPE tissue digests collected from African-American (AFR, n=3) and European-American (EUR, n=3) women. Data reflects sum intensity of the top five most abundant y-ions measured by peptide tandem mass spectrometry and triplicate, technical replicate injections. “NQ” = not quantified. A: Relative abundance of SERPINA1-V237A pAIM heavy SIS and endogenous peptides in AFR and EUR patient tissues. B: A: Relative abundance of CPPED1-A19D pAIM (R.TL(D)AFPAEK) candidates heavy SIS and endogenous peptides in AFR and EUR patient tissues.

Supplemental Tables

Supplemental Table 1A – Peptide Ancestry Informative Markers. Column headers denote the following ProteinAccession_pAIM: Refseq protein accession and missense substitution and amino acid position encoded by the nonsynonymous single nucleotide variant encoding pAIM, SNP-ID: chromosome and genomic loci (hg19), GeneSymbol: Gene name, rsID: reference SNP, VAR_Position: amino acid and position of the reference and variant, AF-African: pAIM allele frequency in African reference populations (1000 genomes project), AF-European: pAIM allele frequency in European reference populations (1000 genomes project), AF-EastAsian: pAIM allele frequency in East Asian reference populations (1000 genomes project), SIFT-D: YES=SIFT score for rsID is predicted to be deleterious by the Variant Effect Predictor tool (Ensembl), PROVEAN-D: YES=PROVEAN score is predicted to be deleterious by the Variant Effect Predictor tool (Ensembl), PolyPhenHVAR=D: YES=PolyPhenHVAR score is predicted to be deleterious by the Variant Effect Predictor tool (Ensembl), Clinical_Significance (CLINVAR): clinical significance for rsID (CLINVAR/ Variant Effect Predictor tool), Trait (CLINVAR): clinical trait correlating with rsID (CLINVAR/ Variant Effect Predictor tool), HS: heterozygosity of the subpopulation, HT: heterozygosity of the total population, FST: fixation index.

Supplemental Table 1B – Peptide Ancestry Informative Markers – Functional enrichment analyses (metascape.org).

Supplemental Table 2 – pAIMs Quantified and genotype for rsID encoding pAIM - Endometrial cancer cell Lines (n=13). UniprotAccMatch: Alternate protein accessions mapping to pAIMs (Uniprot.org). GT: genotype, GT=1_1 (homozygous for variant encoding pAIM), GT=0_1 (heterozygous for pAIM), GT=0_0 (homozygous for reference).

Supplemental Table 3 – pAIMs Quantified - Uterine Leiomyomas (Discovery, n=66). UniprotAccMatch: Alternate protein accessions mapping to pAIMs (Uniprot.org).

Supplemental Table 4 – pAIMs Quantified and genotype for rsID encoding pAIM - Uterine Leiomyomas (Discovery, n=26). UniprotAccMatch: Alternate protein accessions mapping to pAIMs (Uniprot.org). GT: genotype, GT=1_1 (homozygous for variant encoding pAIM), GT=0_1 (heterozygous for pAIM), GT=0_0 (homozygous for reference).

Supplemental Table 5 – Parallel reaction monitoring assay of SERPINA1-V237A and CPPED1-A19D pAIM variants. Table details the dot product similarity (dotp) as well as sum intensities for the top five y-ions quantified by targeted, tandem mass spectrometry for endogenous as well as stable isotope standard (Heavy SIS) peptides in triplicate, technical replicate injections of fibroid FFPE tissue digests from African-American (n=3) and European-American (n=3) women.

Figure 1

A

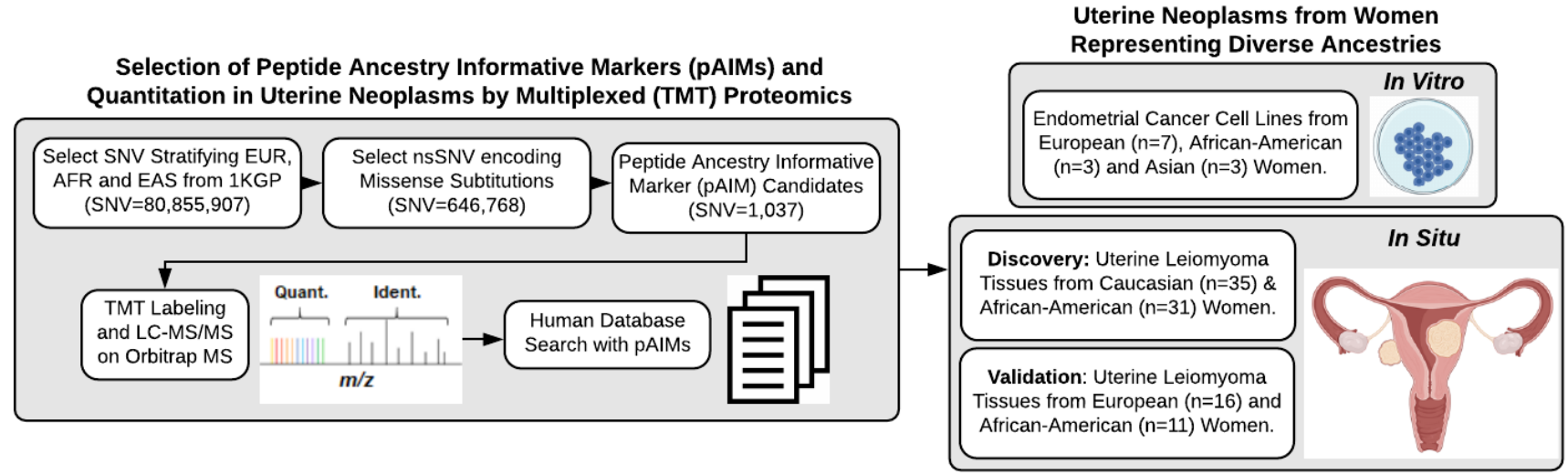
Selection of Peptide Ancestry Informative Markers (pAIMs) and Quantitation in Uterine Neoplasms by Multiplexed (TMT) Proteomics
Select SNV Stratifying EUR, AFR and EAS from 1KGP (SNV=80,855,907)
Select nsSNV encoding Missense Subtitutions (SNV=646,768)
Peptide Ancestry Informative Marker (pAIM) Candidates (SNV=1,037)
TMT Labeling and LC-MS/MS on Orbitrap MS
Quant.
Ident.
m/z
Human Database Search with pAIMs
Uterine Neoplasms from Women Representing Diverse Ancestries
In Vitro
Endometrial Cancer Cell Lines from European (n=7), African-American (n=3) and Asian (n=3) Women.
In Situ
Discovery: Uterine Leiomyoma Tissues from Caucasian (n=35) & African-American (n=31) Women.
Validation: Uterine Leiomyoma Tissues from European (n=16) and African-American (n=11) Women.

Figure 1

B

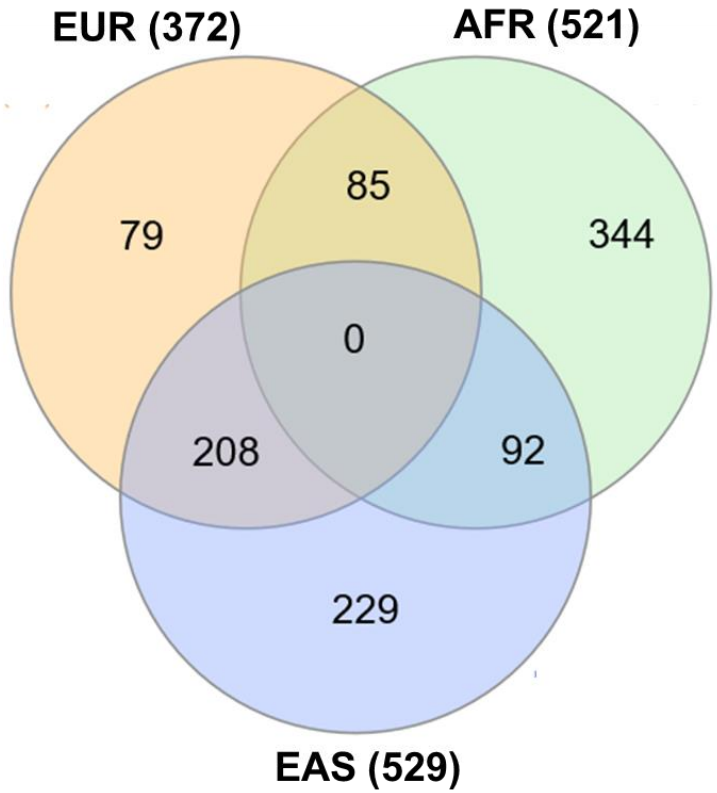

Figure 2

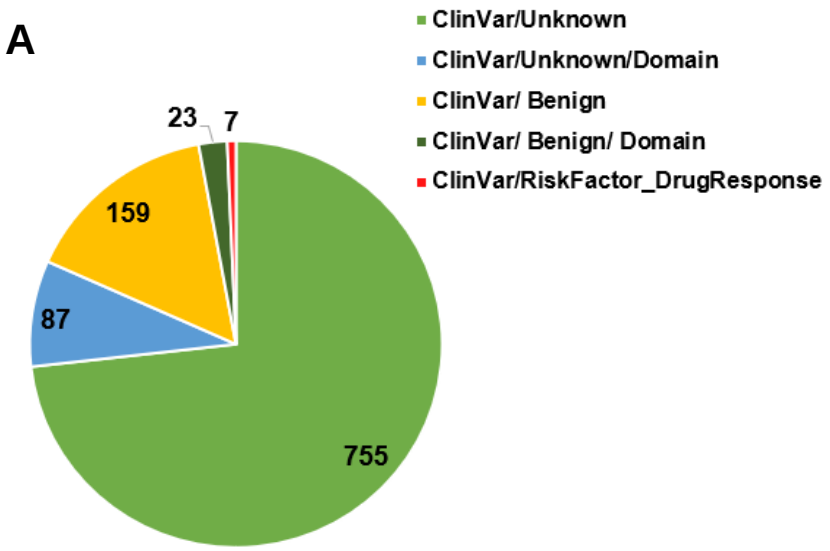
A
ClinVar/Unknown
ClinVar/Unknown/Domain
ClinVar/ Benign
ClinVar/ Benign/ Domain
ClinVar/RiskFactor_DrugResponse
23
7
159
87
755

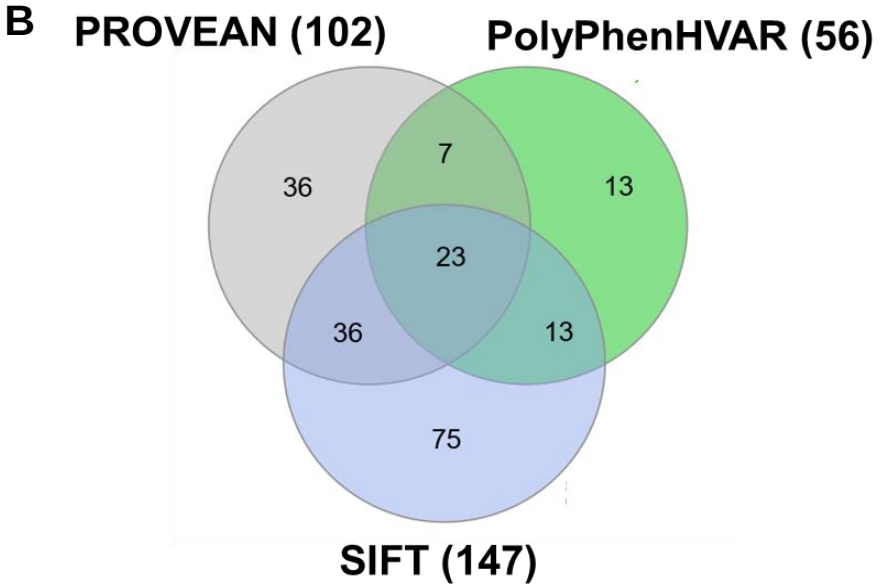
B
PROVEAN (102)
PolyPhenHVAR (56)
SIFT (147)
36
7
13
23
36
13
75

Figure 2

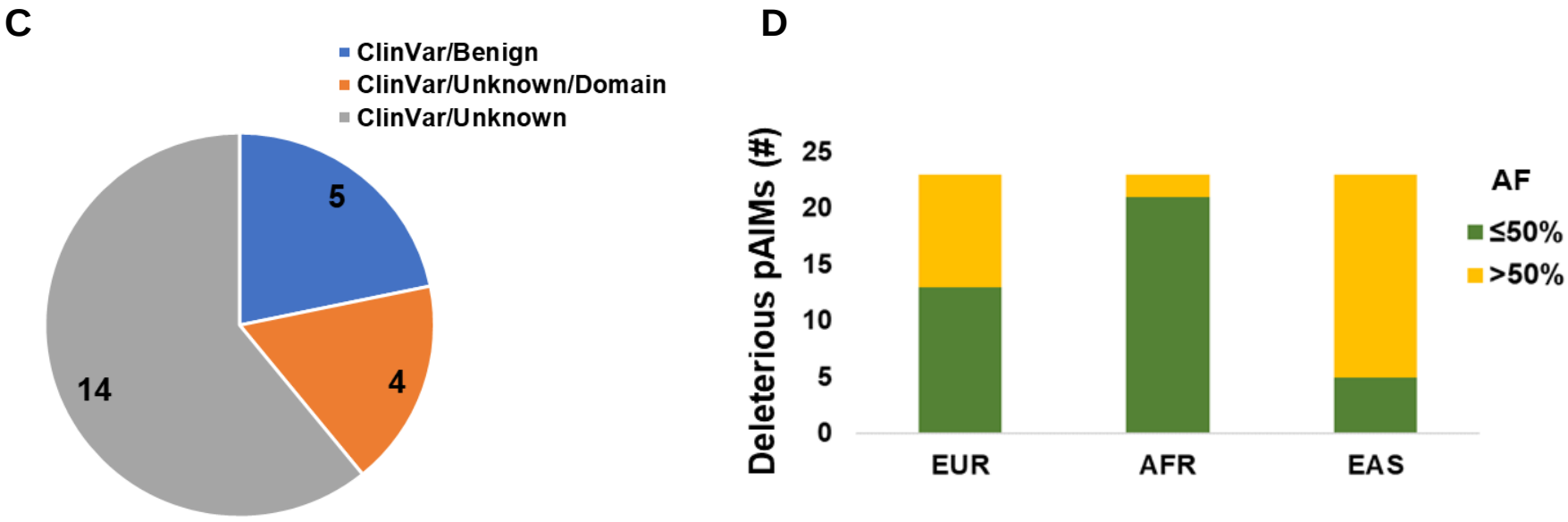
C
ClinVar/Benign
ClinVar/Unknown/Domain
ClinVar/Unknown
5
4
14
D
Deleterious pAIMs (#)
25
20
15
10
5
0
EUR
AFR
EAS
AF
≤50%
>50%

Figure 3

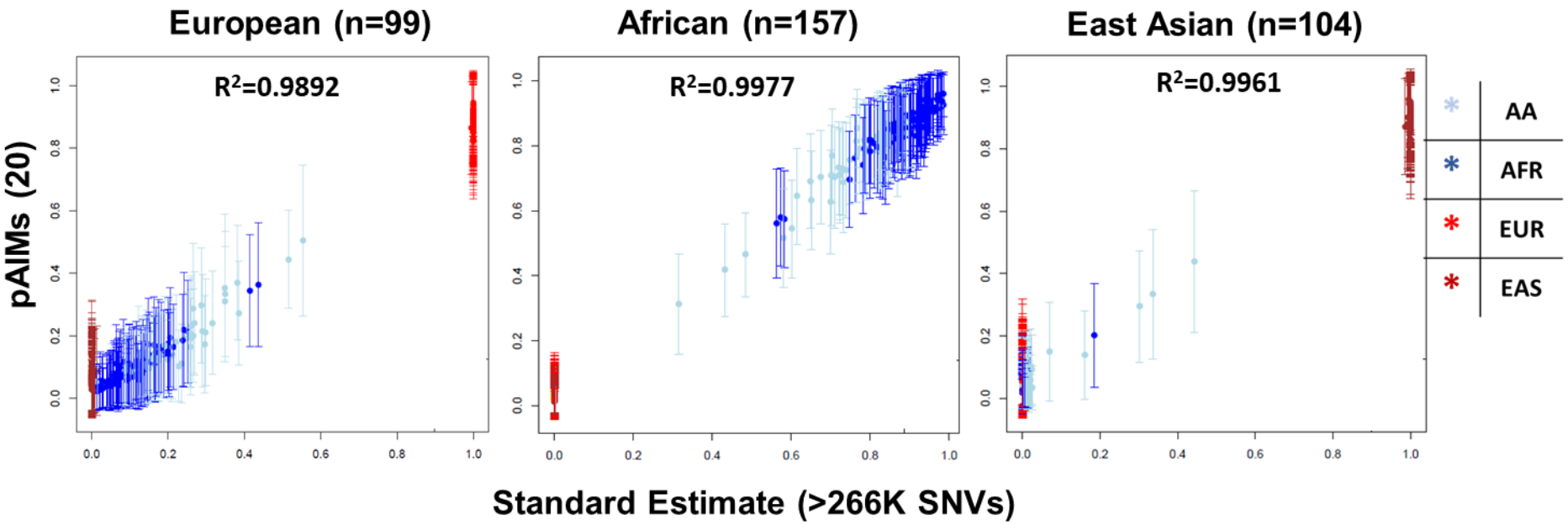
European (n=99)
African (n=157)
East Asian (n=104)
R²=0.9892
R²=0.9977
R²=0.9961
pAIMs (20)
Standard Estimate (>266K SNVs)
AA
AFR
EUR
EAS

Figure 4

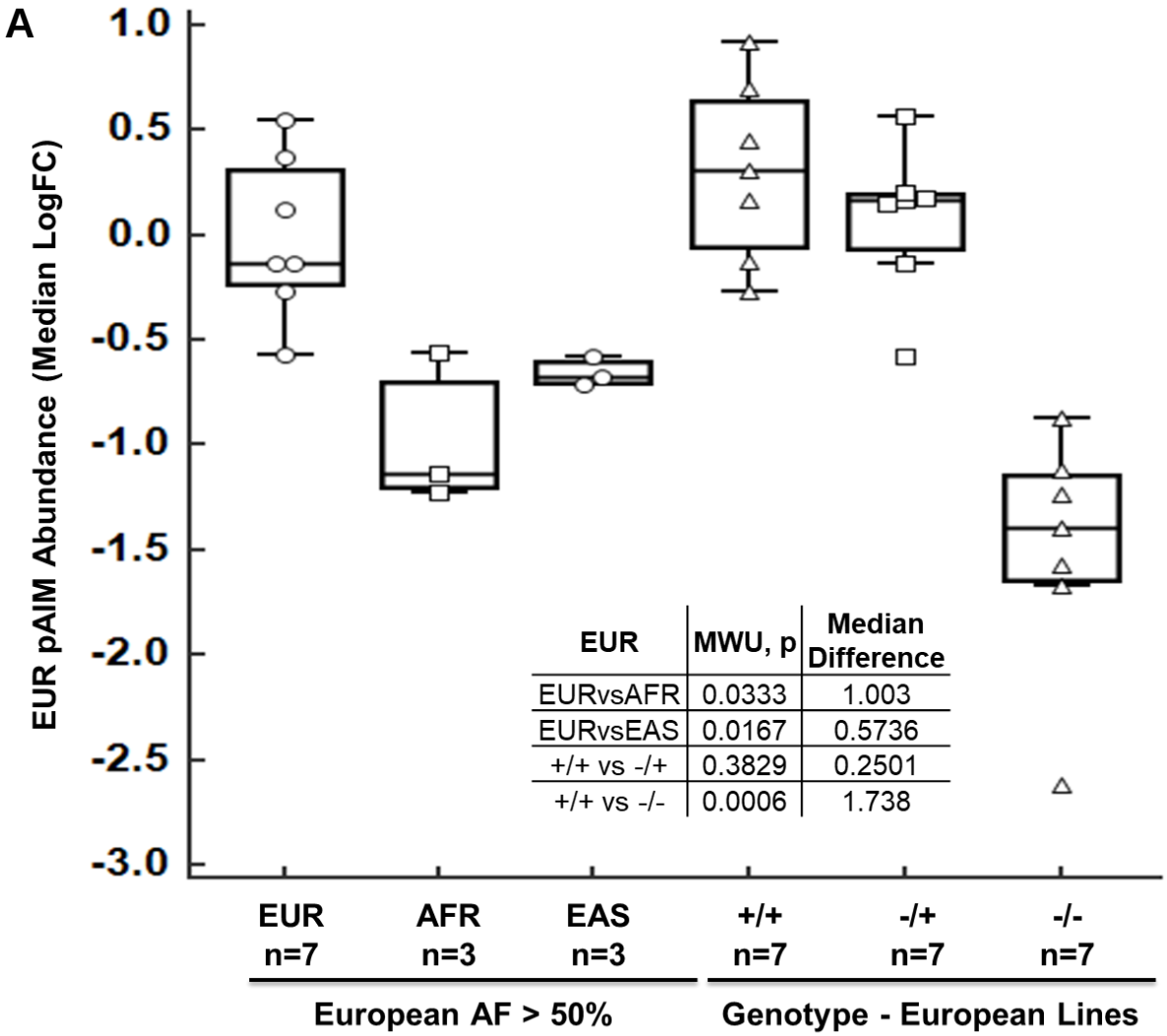

EUR	MWU, p	Median Difference
EURvsAFR	0.0333	1.003
EURvsEAS	0.0167	0.5736
+/+ vs -/+	0.3829	0.2501
+/+ vs -/-	0.0006	1.738

Figure 4

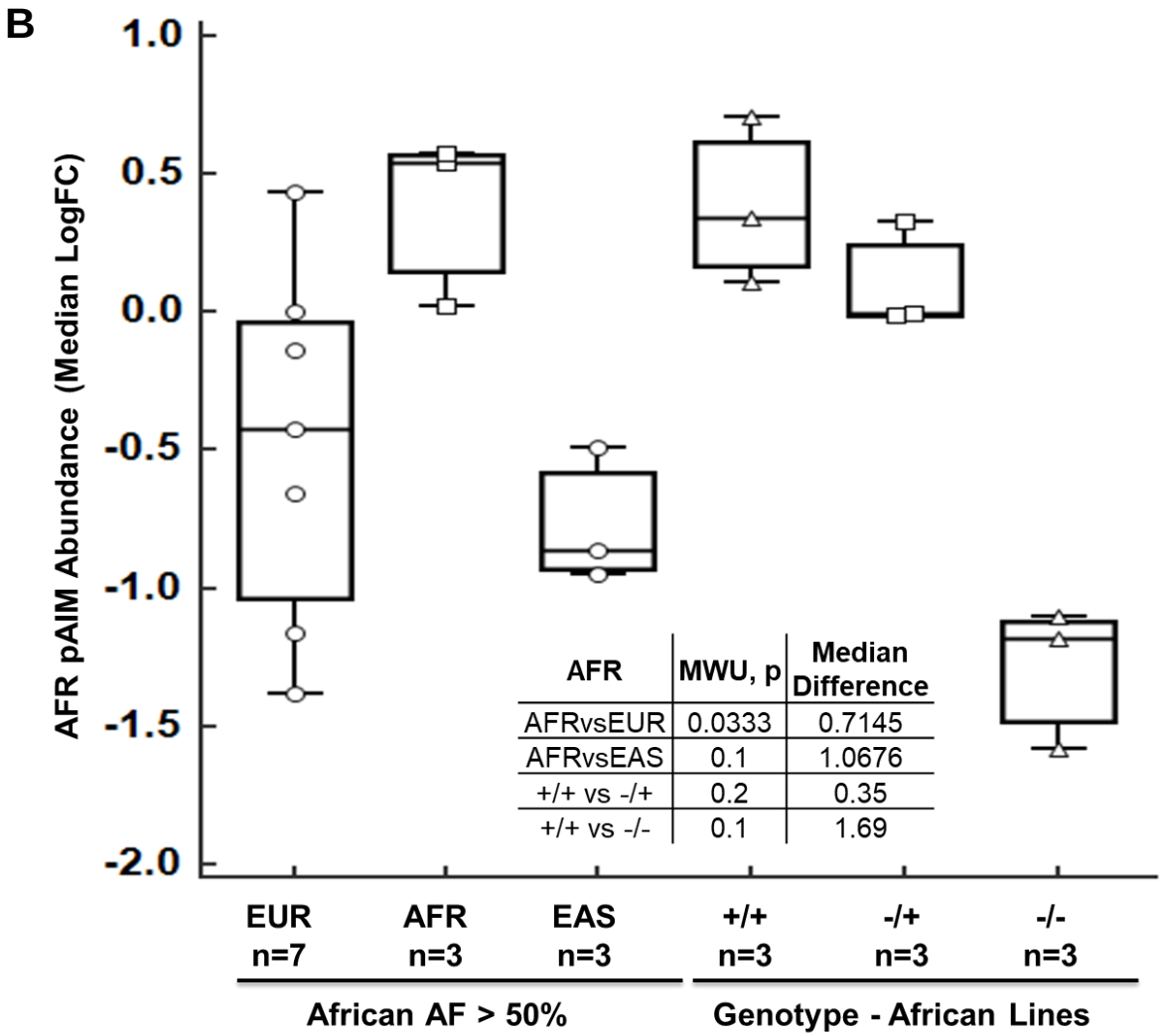

AFR	MWU, p	Median Difference
AFRvsEUR	0.0333	0.7145
AFRvsEAS	0.1	1.0676
+/+ vs -/+	0.2	0.35
+/+ vs -/-	0.1	1.69

Figure 4

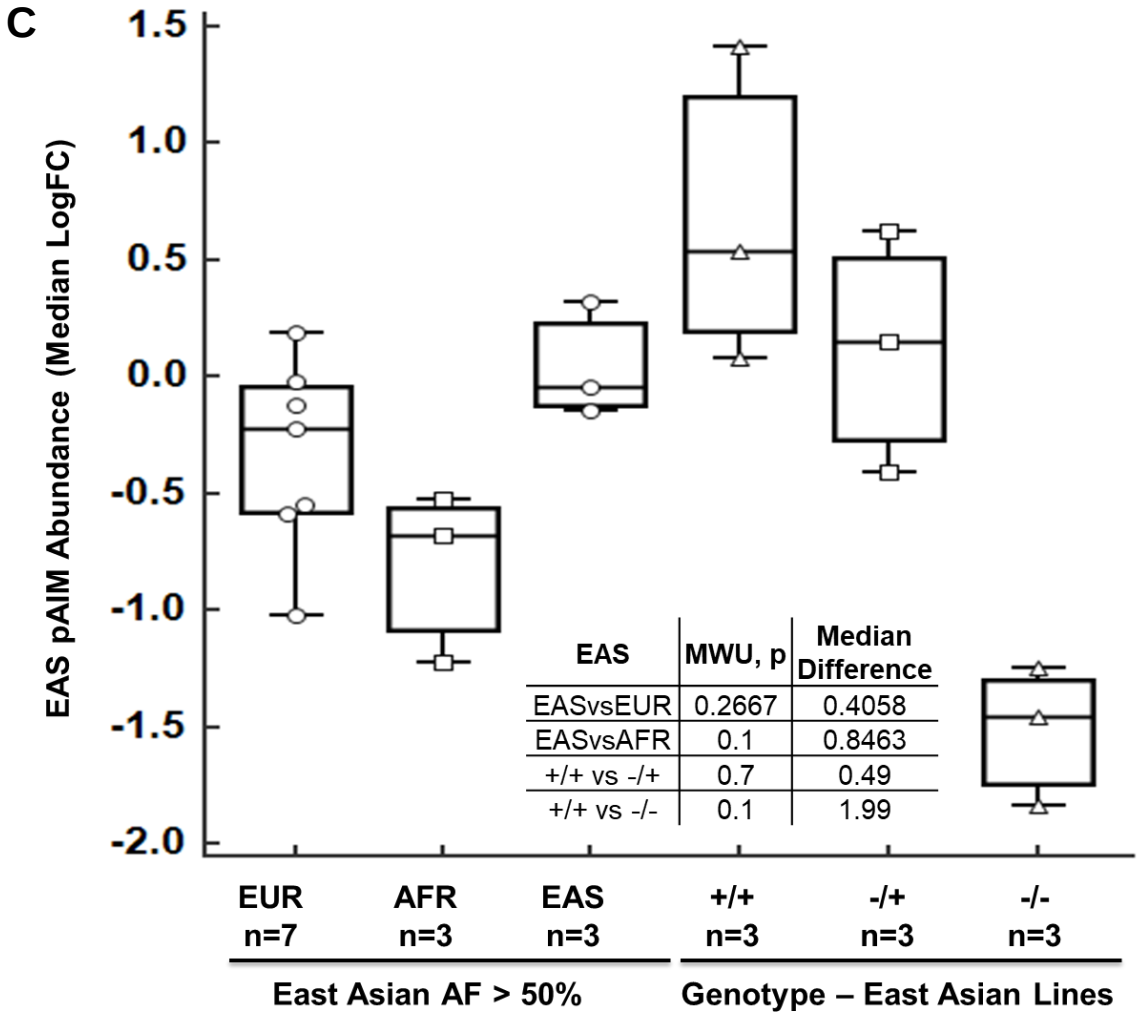

EAS	MWU, p	Median Difference
EASvsEUR	0.2667	0.4058
EASvsAFR	0.1	0.8463
+/+ vs -/+	0.7	0.49
+/+ vs -/-	0.1	1.99

Figure 5

A

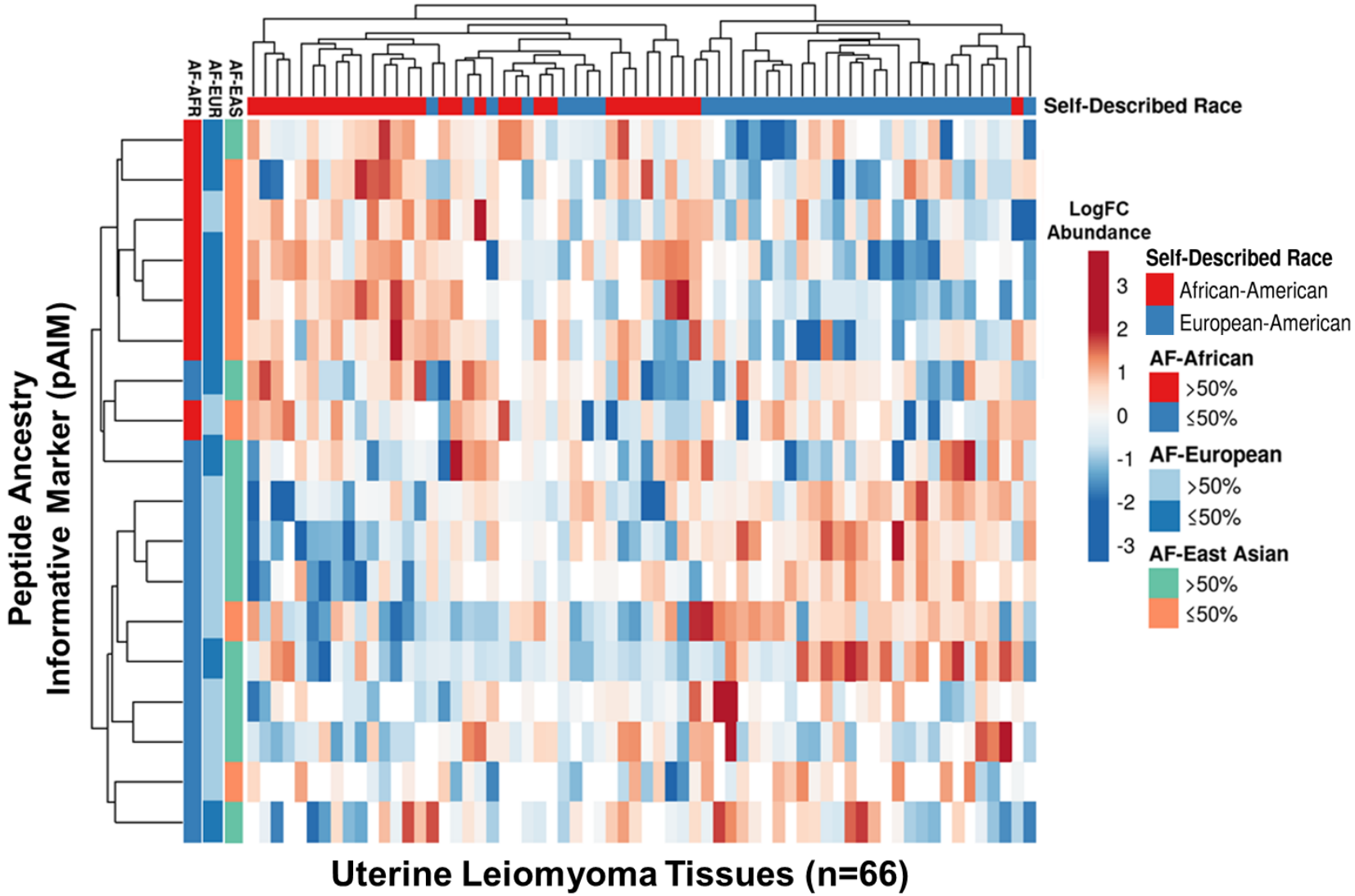
AF-AFR
AF-EUR
AF-EAS
Self-Described Race
Peptide Ancestry Informative Marker (pAIM)
Uterine Leiomyoma Tissues (n=66)
LogFC Abundance
3
2
1
0
-1
-2
-3
Self-Described Race
African-American
European-American
AF-African
>50%
≤50%
AF-European
>50%
≤50%
AF-East Asian
>50%
≤50%

Figure 5

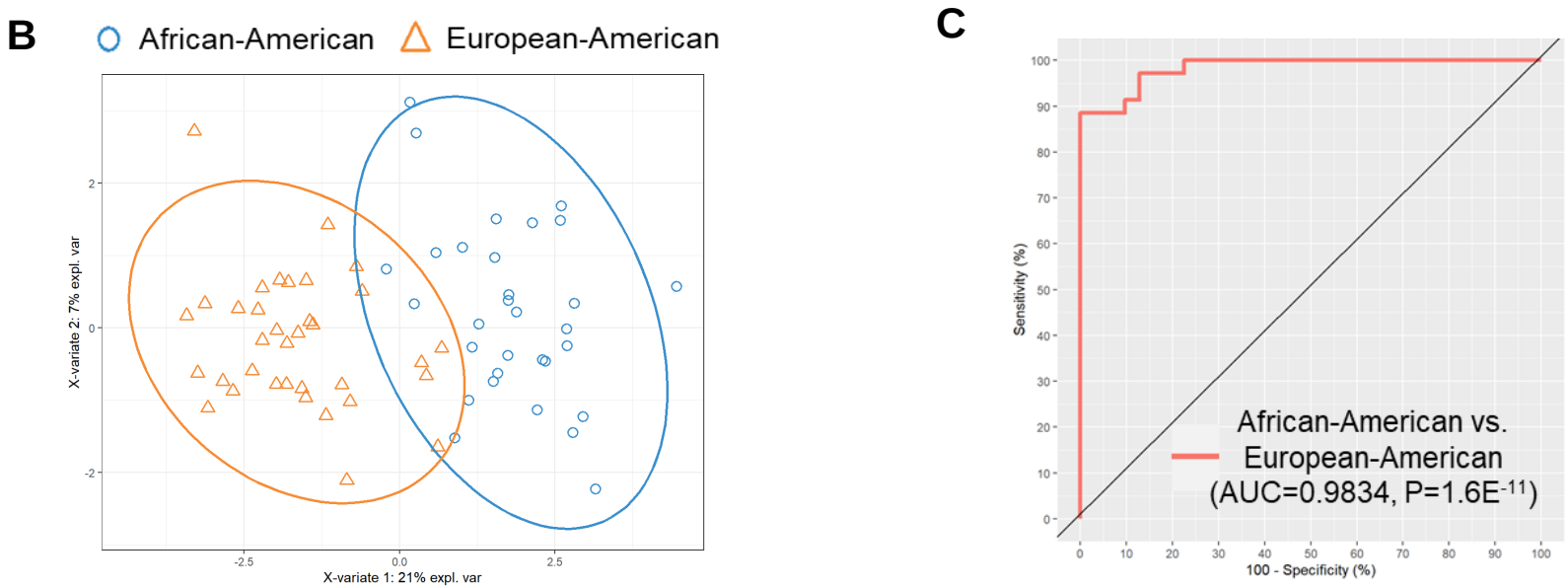
B
African-American
European-American
X-variate 2: 7% expl. var
X-variate 1: 21% expl. var
2
0
-2
-2.5
0.0
2.5
C
Sensitivity (%)
100 - Specificity (%)
African-American vs.
European-American
(AUC=0.9834, P=1.6E-11)

Figure 6

A

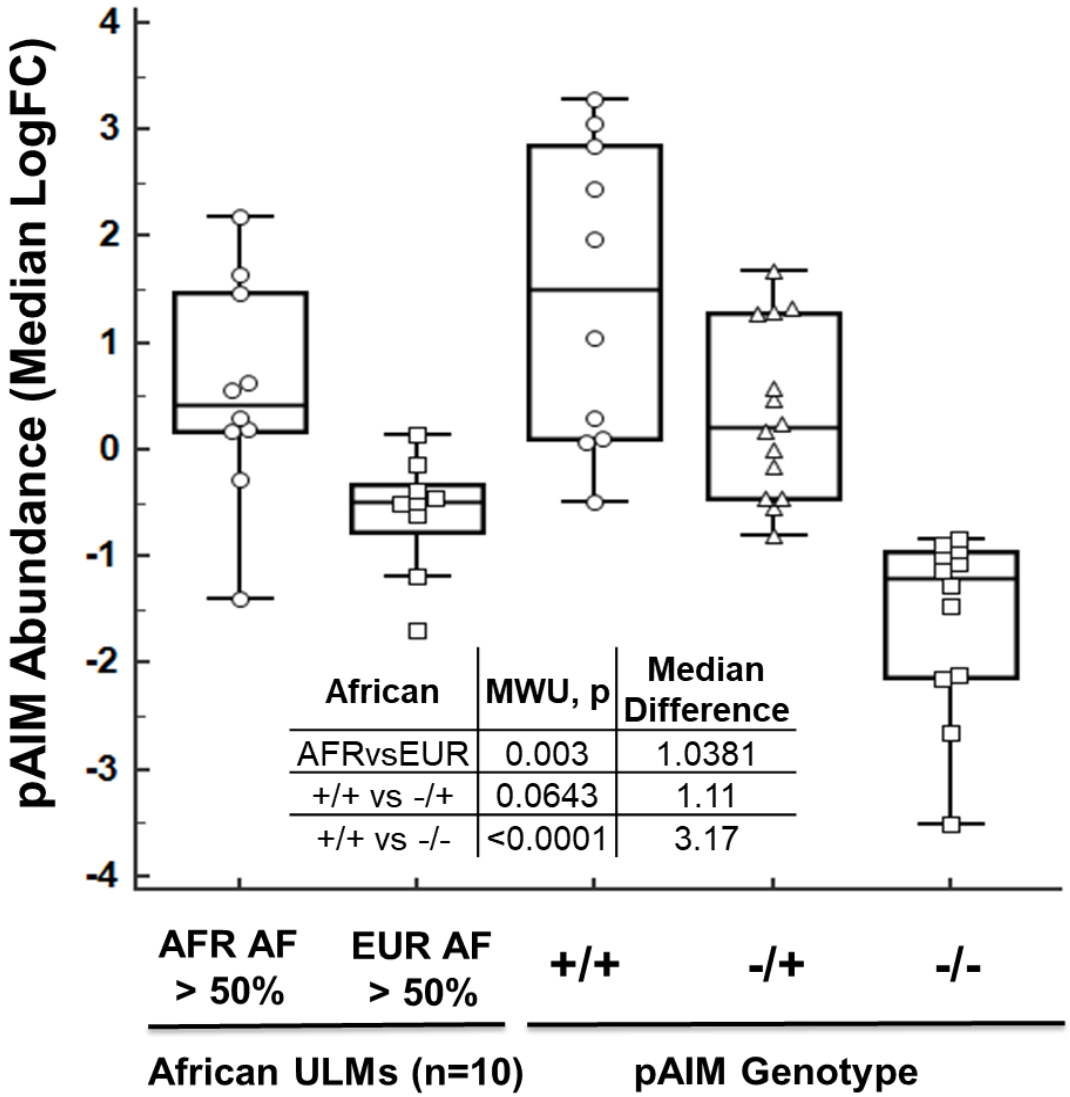
pAIM Abundance (Median LogFC)
4
3
2
1
0
-1
-2
-3
-4
African
MWU, p
Median Difference
AFRvsEUR
0.003
1.0381
+/+ vs -/+
0.0643
1.11
+/+ vs -/-
<0.0001
3.17
AFR AF > 50%
EUR AF > 50%
+/+
-/+
-/-
African ULMs (n=10)
pAIM Genotype

Figure 6

B

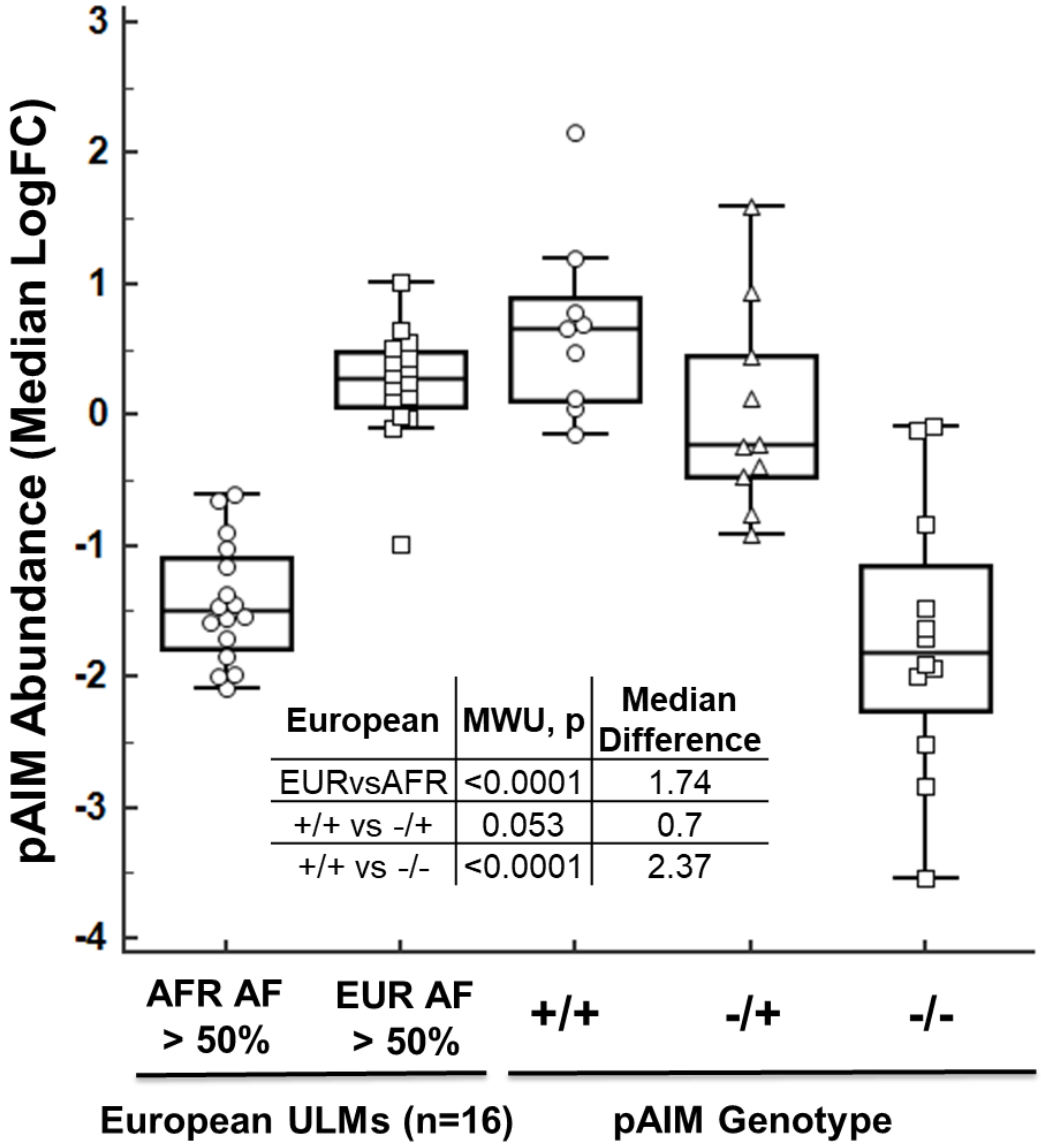

European	MWU, p	Median Difference
EURvsAFR	<0.0001	1.74
+/+ vs -/+	0.053	0.7
+/+ vs -/-	<0.0001	2.37

Figure 7

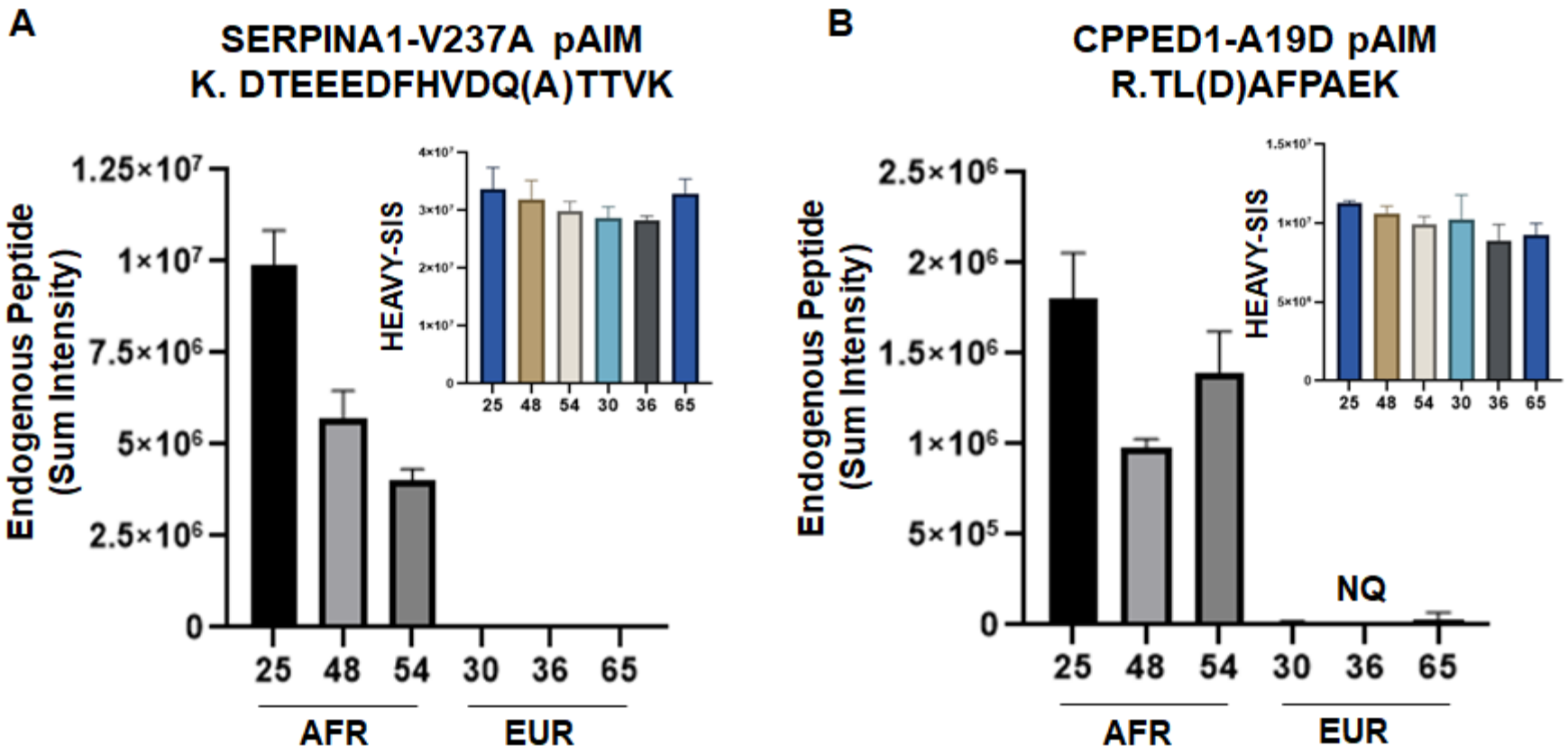
A
SERPINA1-V237A pAIM
K. DTEEEDFHVDQ(A)TTVK
Endogenous Peptide (Sum Intensity)
1.25×10^7
1×10^7
7.5×10^6
5×10^6
2.5×10^6
0
25 48 54 30 36 65
AFR
EUR
HEAVY-SIS
4×10^7
3×10^7
2×10^7
1×10^7
0
25 48 54 30 36 65
B
CPPED1-A19D pAIM
R.TL(D)AFPAEK
Endogenous Peptide (Sum Intensity)
2.5×10^6
2×10^6
1.5×10^6
1×10^6
5×10^5
0
NQ
25 48 54 30 36 65
AFR
EUR
HEAVY-SIS
1.5×10^7
1×10^7
5×10^6
0
25 48 54 30 36 65